AD_____

AWARD NUMBER DAMD17-96-1-6141

TITLE: Characterization of Two Proteins which Interact with the BRCA1 Gene

PRINCIPAL INVESTIGATOR: Frank J. Rauscher, Ph.D.

CONTRACTING ORGANIZATION: Wistar Institute
Philadelphia, Pennsylvania 19104-4268

REPORT DATE: June 1998

TYPE OF REPORT: Annual

PREPARED FOR: Commander
U.S. Army Medical Research and Materiel Command
Fort Detrick, Maryland 21702-5012

DISTRIBUTION STATEMENT: Approved for public release;
distribution unlimited

The views, opinions and/or findings contained in this report are
those of the author(s) and should not be construed as an official
Department of the Army position, policy or decision unless so
designated by other documentation.

1998 0918 031

REPORT DOCUMENTATION PAGE		Form Approved OMB No. 0704-0188

Public reporting burden for this collection of information is estimated to average 1 hour per response, including the time for reviewing instructions, searching existing data sources, gathering and maintaining the data needed, and completing and reviewing the collection of information. Send comments regarding this burden estimate or any other aspect of this collection of information, including suggestions for reducing this burden, to Washington Headquarters Services, Directorate for Information Operations and Reports, 1215 Jefferson Davis Highway, Suite 1204, Arlington, VA 22202-4302, and to the Office of Management and Budget, Paperwork Reduction Project (0704-0188), Washington, DC 20503.

1. AGENCY USE ONLY *(Leave blank)*	2. REPORT DATE June 1998	3. REPORT TYPE AND DATES COVERED Annual (1 Jun 97 - 31 May 98)	
4. TITLE AND SUBTITLE Characterization of Two Proteins which Interact with the BRCA1 Gene			**5. FUNDING NUMBERS** DAMD17-96-1-6141
6. AUTHOR(S) Frank J. Rauscher, Ph.D.			
7. PERFORMING ORGANIZATION NAME(S) AND ADDRESS(ES) Wistar Institute Philadelphia, Pennsylvania 19104-4268			**8. PERFORMING ORGANIZATION REPORT NUMBER**
9. SPONSORING / MONITORING AGENCY NAME(S) AND ADDRESS(ES) U.S. Army Medical Research and Materiel Command Fort Detrick, Maryland 21702-5012			**10. SPONSORING / MONITORING AGENCY REPORT NUMBER**

11. SUPPLEMENTARY NOTES

12a. DISTRIBUTION / AVAILABILITY STATEMENT Approved for Public Release; Distribution Unlimited	12b. DISTRIBUTION CODE

13. ABSTRACT *(Maximum 200 words)*

The functions and the intracellular localization of the breast/ovarian susceptibility gene product, BRCA1, has been controversial. To arrive at a clear understanding of its localization and relative position to other nuclear structures, a new monoclonal antibody was produced and characterized by immunohistochemical techniques with other BRCA1 antibodies. Each of the antibodies specifically detected BRCA1, in a variety of cells and in a cell cycle-dependent manner, localized to specific nuclear domains. However, all antibodies also cross-reacted with the centrosomal domain suggesting that BRCA1 is also localized to this important mitotic component. We found that the BRCA1 containing nuclear domains are different than any of the well defined nuclear domains. However, a cell cycle-related partial overlap was found for HP1a, a chromodomain-containing protein involved in heterochromatin maintenance. Cellular stimuli, such as heat shock and herpesvirus infection, dispersed BRCA1 from its domains. However, infection with Adenovirus 5 recruited BRCA1 to regions of viral transcription and replication. These disparate distributions of BRCA1 may provide clues to its function.

14. SUBJECT TERMS Breast Cancer			15. NUMBER OF PAGES 44
			16. PRICE CODE
17. SECURITY CLASSIFICATION OF REPORT Unclassified	18. SECURITY CLASSIFICATION OF THIS PAGE Unclassified	19. SECURITY CLASSIFICATION OF ABSTRACT Unclassified	20. LIMITATION OF ABSTRACT Unlimited

NSN 7540-01-280-5500

Standard Form 298 (Rev. 2-89)
Prescribed by ANSI Std. Z39-18 298-102

USAPPC V1.00

FOREWORD

Opinions, interpretations, conclusions and recommendations are those of the author and are not necessarily endorsed by the U.S. Army.

_____ Where copyrighted material is quoted, permission has been obtained to use such material.

_____ Where material from documents designated for limited distribution is quoted, permission has been obtained to use the material.

_____ Citations of commercial organizations and trade names in this report do not constitute an official Department of Army endorsement or approval of the products or services of these organizations.

_____ In conducting research using animals, the investigator(s) adhered to the "Guide for the Care and Use of Laboratory Animals," prepared by the Committee on Care and Use of Laboratory Animals of the Institute of Laboratory Resources, National Research Council (NIH Publication No. 86-23, Revised 1985).

_____ For the protection of human subjects, the investigator(s) adhered to policies of applicable Federal Law 45 CFR 46.

_____ In conducting research utilizing recombinant DNA technology, the investigator(s) adhered to current guidelines promulgated by the National Institutes of Health.

_____ In the conduct of research utilizing recombinant DNA, the investigator(s) adhered to the NIH Guidelines for Research Involving Recombinant DNA Molecules.

_____ In the conduct of research involving hazardous organisms, the investigator(s) adhered to the CDC-NIH Guide for Biosafety in Microbiological and Biomedical Laboratories.

PI - Signature   6/26/98   Date

CHARACTERIZATION OF TWO PROTEINS WHICH INTERACT WITH
THE BRCA1 GENE

TABLE OF CONTENTS

Introduction

The identification of the breast cancer susceptibility gene BRCA1 (1) has triggered an intensive search for its function. Much of this search has focused on the identification of interacting proteins and has yielded components of the nuclear import pathway (2), and a novel RING finger containing protein BARD1 (3, 4). Recently, we identified the BRCA1-associated protein BAP1 (5 and see appendix) which is a nuclear localized ubiquitin hydrolase, suggesting that BRCA1 functions may be either mediated or regulated through ubiquitination-related modifications. Biological clues to BRCA1's function(s) has come through over- or under-expression studies. A reduction in BRCA1 availability by antisense expression yielded transformed fibroblasts and accelerated growth of breast cancer cell lines (6, 7), whereas over-expression of wild-type BRCA1 inhibited colony formation and tumor growth in vivo. The observations are consistent with the genetic evidence that BRCA1 functions as a tumor suppressor (8; 5). BRCA1 also seems to be associated with the DNA recombination/repair protein RAD51 in meiotic cells (9) suggesting involvement of BRCA1 in the fidelity of DNA replication.

The BRCA1 gene encodes an 1863 amino acid protein of ~220 kDa which is predominately found within the nucleus (4, 10), although some investigators have observed cytoplasmic localization (11, 12). The BRCA1 protein contains two highly conserved regions, one at the amino terminus and the other at the C-terminus. The C-terminus contains an acidic region and two copies of a novel motif, designated the BRCT domain. The BRCT domain is present in a variety of putative cell-cycle related proteins, including RAD9, 53BP1 (13) as well as the BRCA1-associated protein BARD1 (3). The BRCA1 C-terminal domain is capable of activating transcription as a Gal4 DNA-binding domain fusion (14) suggesting a role for BRCA1 in transcriptional regulation. The co-fractionation of BRCA1 with the RNA pol II holoenzyme (15)supports this hypothesis. However, not all of the BRCA1 co-fractionates with pol II, suggesting multiple functions for BRCA1.

The amino terminal region is a 100 amino acid sequence encoding a RING finger domain, which is predicted to bind zinc (16, 17). This motif is defined by a spatially conserved set of cysteine-histidine residues of the form C3HC4 (for reviews, see; 18, 19). The RING motif occurs in over 80 proteins including the products of proto-oncogenes and putative transcription factors (19) and may function as a protein-protein interface. Evidence for this hypothesis has come from the study of the proto-oncogene PML (16), the transcriptional co-repressor KAP-1 (20), and a ubiquitin hydrolase, BAP1 (5).

The abundance and intracellular location of BRCA1 varies with the cell-cycle. BRCA1 protein levels are low in G1 phase and reach a maximum during S phase, results that are consistent with BRCA1 RNA expression patterns (21-24). Interestingly, the location of BRCA1 within the nucleus seems to vary with the cell cycle. BRCA1 is detected as diffuse immunofluorescent staining throughout the nucleus during G1, but then localizes to discrete nuclear domains during S phase (4, 10). The functional effects of these cellular and biochemical changes remain unknown.

The nucleus is a highly organized structure, not only in the positioning of chromosomes in specific territories but also by the distribution of extrachromosomal domains like the interchromatinic granules recognizable by the location of the spliceosome assembly factor SC35 (25, 26). In addition, coiled bodies were found to be associated with specific genes and snRNA and associated proteins (27-30). PIKA is a nuclear domain that shows cell

cycle associated changes in the aggregation of HP-1 (31). Other specifically circumscribed nuclear domains (ND10) have been described to contain the proto-oncogene product PML as well as Int-6, which, if interrupted in the mouse by a retrovirus, results in mammary tumors (32, 33). Although the biochemical functions of these domains are not known, various nuclear processes like RNA processing (SC35 domain) and initiation of DNA virus replication and transcription (34, 35) occur at these domains. Since BRCA1 is also localized to discrete nuclear domains, potential functions of BRCA1 may be suggested, or excluded, by interaction or co-localization with any of the known nuclear domains. The relative position of BRCA1 in the nucleus may therefore be informative.

Recent findings on nuclear structure and distribution of specific proteins after viral infection showed that some of them are modified at specific stages of viral infection. Instructive are those that appear at very early times of the viral reproductive cycle before nuclear damage becomes apparent and which can be traced to the activity of a specific immediate early protein. The IE1 gene product of herpesvirus type 1 (HSV-1) disperses the ND10 associated proteins (36, 37, 37, 38) and the E4orf3 gene product of adenovirus 5 (Ad5) repositions the same proteins into short tracks (39, 40, 41). We therefore used these viruses to determine if they have any effect on BRCA1 distribution.

The ability to establish co-localization of two proteins by microscopic examination suggested that this methodology should be used as a means to search for other correlations of either the nuclear sites with known functions, or for conditions which change the distribution of BRCA1. We therefore developed a monoclonal antibody that reliably localized BRCA1 relative to different nuclear domains. The results of these experiments clearly show that BRCA1 is a protein with dramatic nuclear repositioning during the cell cycle and upon experimental manipulations of the cell such as stress and viral infection. These changes suggest that adenovirus 5 transcription and replication can provide the experimental system to help elucidate BRCA1 functions.

Body

I. Materials and Methods

Cell Culture: All cells were maintained at 37°C and 5% CO_2. MCF7 cells (ATCC HTB 22) and HBL-100 (ATCC HTB 124) cells were grown in high glucose DMEM containing 10% FBS and 0.1mM non-essential amino acids. MDA-MB-468 (ATCC HTB 132) cells were grown in a 1:1 mix of high glucose DMEM and Hams F-12 with 10% FBS. Human WI38 fibroblasts (ATCC CCL 75) and the epithelial cell line HEp-2 (ATCC CCL 23), were maintained in MEM supplemented with 10% FCS and antibiotics.

$^{32}PO_4$ **labeling of MDA-MB-468 cells:** MDA-MB-468 cells were rinsed twice with warm, phosphate-free DMEM (hi glucose) medium and then incubated in phosphate-free medium containing 5% dialyzed FBS for 2 hrs. The cells were then placed in phosphate-free medium containing 5% dialyzed FBS and $^{32}PO_4$ (100 uCi/mL; NEN) and incubated for a further 2 hours. Cells were harvested in RIPA buffer containing 50 mM NaF and protease inhibitors (20 mM Hepes, pH 7.4, 140 mM NaCl, 1% Triton

X100, 1% deoxycholate, 0.1% SDS, 1 mM EDTA, 1mM PMSF, 2ug/mL Leupeptin, 0.04 TI units/mL Aprotinin and 2ug/mL Pepstatin).

Monoclonal antibody production: A synthetic gene of the BRCA1-RF domain (amino acids 1-100) was made from overlapping oligonucleotides whose codon usage had been optimized for expression in E.coli and S. cerevisiae (5, 58). Double-stranded DNA was generated by the Polymerase Chain Reaction (PCR). This BRCA1 partial cDNA was fused downstream of the 6 Histidine residues of the vector pQE-30 (QIAGEN Inc.). The His-tagged protein was purified from *E.coli* over a Ni-agarose column as previously described (20). 50 mg recombinant 6XHis-BRCA1 fusion protein, in 50 ml PBS, was emulsified in complete Freund' adjuvant and injected s.c. into Balb/c mice followed by 3 boosts in incomplete Freund adjuvant. The 4th boost was given i.v. and the splenocytes were fused three days later with the mouse non-Ig secreting cell line P3X63Ag8.SP2/0. Hybridomas were selected by testing supernatants by Elisa on recombinant 6XHis-BRCA1. Each clone was subcloned following standard procedures. All resulting monoclonal antibodies were of IgG1, kappa.

Immunoprecipitations: Immunoprecipitation of samples with polyclonal Abs was performed with Protein A Sepharose (Pharmacia). The monoclonal antibody BR64 was precipitated with Protein G Sepharose (Pharmacia). Immunoprecipitations were carried out by incubating the antibody with protein extract or *in vitro*-produced protein in 1 mL of RIPA buffer for 2 hours at 4°C. The protein G (or A) sepharose resin was then added and the reaction incubated a further 30-45 mins. at 4°C with continual mixing. The bound proteins were washed in RIPA buffer 5 times, released from the sepharose resin with SDS-PAGE loading dye and separated by SDS-PAGE. Visualization of bound protein was performed by autoradiography.

Western Blot Analysis: Proteins were separated by SDS-PAGE and transferred to PVDF membrane (Millipore) via standard methods. The membrane was blocked in Tris-buffered Saline containing 0.1% Tween-20 (TBST) and 5% fish gelatin (Forma Scientific). The MAb BR64 ascitis fluid was diluted 1:1000 in the block buffer and incubated with the membrane for 2 hours at room temperature with gentle shaking. After washing the membrane 5 times with TBST (10 minutes each), the blot was incubated with secondary antibody conjugated to horse radish peroxidase (goat anti-mouse IgG-HRP; BioRad) at 1:5000 dilution for 30 minutes. The membrane was washed 5 times further and developed with Super Signal (Pierce). The membrane was blocked for 1 hour in Tris-buffered Saline containing 0.2% Tween-20 (TBST2) and 5% dry milk. The MAb BR64 ascitis fluid was diluted to 0.5 ug/mL (TBST2 plus 1% BSA) and incubated with the membrane for 1 hour at room temperature with gentle shaking. After washing the membrane 3 times with TBST2 (10 minutes each), the blot was incubated with secondary antibody conjugated to alkaline phosphatase (alkaline phosphatase anti-mouse IgG; Promega) at 1:7500 dilution (TBST2 plus 1% BSA) for 45 minutes. The membrane was washed 3 times further and developed using BCIP/NBT color development substrates (Promega).

Transfections and *in vitro* Transcription/Translation: Cells were transiently transfected by Ca-phosphate precipitation (59). The Promega TNT kit was used as described by the manufacturer to produce ^{35}S-labeled protein. Proteins were used for

4

analysis without further purification.   Plasmid constructs bearing BRCA1 and BRCA1-D11 were kind gifts of F. Calzone.   The RPT-1 cDNA was a kind gift of H. Cantor (44).

Antibodies used for Immunofluorescense

Antibodies used for the detection of BRCA1 were: M13, a monoclonal antibody (MAb) kindly provided by R. Scully (60). 17F8, a Mab kindly provided by W.H. Lee (11); and C20, a rabbit polyclonal antibody which was purchased from Santa Cruz Biotechnologies (Paolo Alto, CA).

ND10 were visualized using Mab 1150, which recognizes Sp100 (61). The human antibody 1745, which recognizes Sp100 and PML was used in triple-labeling experiments (61). MAb anti-SC35 (25) were used to label the SC35 domain. Isotype-matched MAbs of unrelated specificity served as controls. Rabbit anti-HP1a antibodies were obtained from W. Earnshaw (31).

Immunohistochemistry. Cells were fixed at room temperature for 15 min. with freshly prepared 1% paraformaldehyde in PBS, washed with PBS, and permeabilized for 20 min. on ice with 0.2% (v/v) Triton X-100 (Sigma Chemical Co.) in PBS.   Antigen localization was determined after incubation of permeabilized cells with rabbit antiserum, MAb or human antiserum diluted in PBS for 1 h at room temperature.   Avidin-fluorescein or avidin-Texas Red was complexed with primary antibodies through biotinylated secondary antibodies (Vector Laboratories).   Cells were double- or triple-labeled with the respective second antibodies conjugated with FITC, Texas Red, or Cy-5 using biotin-avidin enhancement and FITC for structures with the lowest staining intensity.   Cells were then stained for DNA with 0.5 mg/ml of bis-benzimide (Hoechst 33258; Sigma) in PBS and mounted with Fluoromount G (Fisher Scientific).   Cells were analyzed using a Leica confocal scanning microscope. The two channels were recorded simultaneously when no cross-talk could was detectable. In the case of intense FITC-labeling, sequential images were acquired with more restrictive filters to prevent possible breakthrough of the FITC signal into the red channel. Both acquisition modes gave the same results. Leica image enhancement software was used in balancing signal strength. Because of the variability of the infectious cycle progression in any given culture, the most prevalent and representative images were photographed and presented as limited number of nuclear images to retain high magnification.   At least of 500 cells were studied in each sample.

Virus Infection.   Two days after plating, HEp-2 cells were infected with HSV-1 17^+ at 2 PFU/cell resulting in 95% infected cells as determined by staining for ICP0 antibodies at 5 h p.i. Cells were fixed at different intervals after infection and assayed with different antibodies as described (34). Ad5 infection was carried out as described (41), and cells were fixed at various times post-infection.

II. Results and Discussion

Characterization of monoclonal antibody BR64.   To determine possible functions for BRCA1, we investigated its subcellular localization and its potential co-localization with a variety of known nuclear proteins of differing function.   Investigation of the subcellular localization of BRCA1 required a well characterized, highly specific antibody.   Towards this end, we developed a monoclonal antibody specific for BRCA1, using the first 100 amino acids of the BRCA1 protein as the antigen (Figure 1A).   This region was expressed in *E.coli* as a histidine fusion protein, purified under denaturing conditions and renatured by dialysis (see Materials and Methods and 20). This purified protein was used as the immunizing agent in mice and monoclonal antibodies produced using standard technology.

Since the immunizing antigen contains the RING finger domain of BRCA1, and since many proteins contain RING domains, we determined the specificity of our monoclonal antibody, termed BR64, for the BRCA1 RING domain versus the RING domains of two other, unrelated proteins; the transcriptional co-repressor KAP-1 and the immediate early protein, ICP0, from herpes simplex virus type I.   Through immunoprecipitation analyses with the BR64 antibody, we found that it detected the BRCA1 RING domain in both the full length protein and the smaller BRCA1-Δ11 protein (an alternatively spliced version of BRCA1; 42), but not either of the other RING domains (Figure 2A), suggesting that the antibody identifies a sequence specific region of BRCA1 rather than a structural component of the RING finger which may be in common with other RING domains.

Mutations occur throughout BRCA1, and most are truncations or nonsense mutations (43).   Given that the epitope of this antibody is at the amino terminus of the protein, it should detect all except the shortest BRCA1 mutant proteins.   Therefore, we characterized whether BR64 could identify BRCA1 protein which contained any one of several mutations previously identified in breast cancer kindreds, focusing on mutations found in the RING domain (Figure 1B).   We used proteins which contained the LexA DNA binding domain fused to: 1) the first 100 amino acids of BRCA1 (BRCA1-RF); 2) this same region but containing a missense mutation in a metal-coordinating cysteine residue (BRCA1-RF(C61G) and BRCA1-RF(C64G)); or 3) a truncated BRCA1-RF containing the appropriate number of amino acids as dictated by the mutation (delAG185 = 29 a.a. and del31 = 31 a.a.).   The RING domain of the T-cell transcription factor RPT-1 (44), the most closely related RING finger sequence, was also included.   Again, immunoprecipitation analysis was used to identify proteins bound by the BR64 antibody (Figure 2B).   The BR64 antibody identified only those proteins which contained the full RING domain region, regardless of the presence or absence of missense mutations (Figure 2B).   Again, these results suggest that the BR64 antibody identifies a sequence specific region of BRCA1, rather than a structural component of the RING finger, since the missense mutations are predicted to abolish the coordination of one of the zinc atoms leading to the disruption of the complex RING structure (16).   The fact that the RING domain of the RPT-1 protein was not identified by BR64 further suggests that the antibody identifies a sequence specific domain within BRCA1.

We determined the subregion within the amino terminal 100 amino acids of BRCA1 which the BR64 monoclonal antibody (MAb) detects. LexA-BRCA1-RF fusion proteins, containing successive 10 amino acid deletions from the carboxy terminus of the 100 amino acid BRCA1 RING finger protein, were immunoprecipitated with the BR64 MAb (Figures 1B and 2C). The BR64 MAb detected the full length RING finger domain (BRCA1(1-100)) and the RING domain truncated by 10 amino acids (BRCA1(1-90)). The 20 and 30 amino acid deletions, BRCA1(1-80) and BRCA1(1-70) were not detected by BR64, clearly indicating that amino acids 80 to 100 contain the region identified by BR64. These immunoprecipitation analyses suggest that the BR64 antibody detects an epitope C-terminal to the C3HC4 motif which defines the RING domain proper.

The ability of BR64 to detect authentic, endogenous BRCA1 protein was determined through three methodologies; Immunoprecipitation, immunoprecipitation followed by western blot analysis, and direct western blot analysis of nuclear extract. That BR64 detected BRCA1 was determined by a comparison of the products immunoprecipitated from whole cell extracts of $^{32}PO_4$-labeled MDA-468 breast cancer cells by the BR64 MAb and the commercially available C20 polyclonal antibody (Figure 3A). Both antibodies identify a 220 kDa phosphoprotein, suggesting that the protein detected by BR64 is BRCA1. Furthermore, BRCA1 is the only phosphoprotein detected by BR64, whereas the C20 antibody detects three other phosphoproteins of 190, 97, and 70 kDa.

A second piece of evidence that the endogenous protein detected by BR64 is BRCA1 was obtained via immunoprecipitation-western analysis (Figure 3B). Whole cell extracts prepared from HBL100 breast cancer cells were immunoprecipitated with either (rabbit) pre-immune serum or anti-BRCA1 immune serum. The immunoprecipitated proteins were then analyzed by western blot. The BR64 MAb detected a protein of 220 kDa previously immuno-precipitated by a specific anti-BRCA1 antibody. However, BR64 also detected a second, faster migrating, protein. To address the possibility that BR64 interacted with another protein of large molecular weight, direct western analysis of nuclear extract from HeLa cells was performed (Figure 3C). The BR64 MAb detected only a single protein of 220 kDa, the size of BRCA1. Taken together, these results show that BR64 identifies only the BRCA1 protein, can identify native and denatured BRCA1 protein and has an epitope defined by amino acids 80 to 100. The faster migrating protein of Figure 3B remains unidentified and is not seen in the IP-western blot analysis when other anti-BRCA1 antibodies are used (data not shown).

Comparison of different BRCA1 antibodies. Initial reports that BRCA1 was localized to the cell membrane and the Golgi apparatus and was perhaps secreted (12) have generated significant controversy. It was therefore essential to test whether the earlier reports could be confirmed with different monoclonal antibodies. When the BR64 MAb was tested by immunohistochemical methods, it reacted nearly exclusively with proteins in the nucleus. However, not all cells showed the same distribution as previously reported by others (10). Nuclei of some cells displayed a sandy fluorescence where as others had, in addition, distinctly higher aggregations of the antigen (Figure 4A). There was a faint background staining over the cytoplasm and often two dots were recognized at the position of the

centrosome (Figure 4A, arrow). Another anti-BRCA1 MAb, M13 (see Materials and Methods), recognized the same nuclear patterns (HEp-2 cells) with slightly elevated cytoplasmic staining. In a few cells, particularly mitotic cells, M13 detected numerous cytoplasmic dots over a strong cytoplasmic background (Figure 4B, arrow). A third anti-BRCA1 MAb, 17F8 (see Materials and Methods), labeled a large number of cytoplasmic dots in all cells. Nuclear staining by this MAb was difficult to distinguish from the cytoplasmic staining, but it appears similar to that of the other two Mabs. In addition, each cell stained by 17F8 contained an area of strong staining that localized to the centromeric region and appeared at times to overlap with the nucleus when imaged in the same optical section (Figure 4C; arrows). A rabbit antibody (C20; Santa Cruz) raised against the C-terminal 20 amino acids of BRCA1, labeled the same nuclear components as all three MAbs (Figure 4D), but also stained the Flemming body (data not shown) and, in a few cells, a limited number of cytoplasmic granules. That the new MAb BR64 recognizes the same nuclear structures as C20 is shown by double labeling (Figure 4H). The BRCA1 distribution detected in HEp-2 cells by these antibodies was also found in the diploid human fibroblast cell line WI38 and the breast cancer cell line HBL100. The different antibodies therefore, recognize the same structural components in the nucleus, but appear to have individual, minor, cross-reactivities. We conclude that, in general, the sandy nuclear staining of some cells and the specific nuclear domain dot-like staining of other cells is similar for all of the antibodies and is therefore considered specific for the location of BRCA1.

Testing these four antibodies on the breast cancer cell line MDA-MB-468 quite different images were prevalent. Only a very small number of these breast cancer cells had any particulate, nuclear BRCA1 staining, although the images presented were selected to contain one nucleus with such staining to show that this distribution can exist in this cell type. BR64, of the four antibodies tested, revealed the same image as expected from the non-breast cancer cells (Figure 4E; arrows point to centrosomes). MAb M13 labeled a particular type of cytoplasmic filament (see arrows; Figure 4F). In mitotic cells these fibers disappeared and resulted in cytoplasmic dots. MAb 17F8 recognized a large cytoplasmic component similar to HEp-2 cells and stained the centrosomes (Figure 4G, arrows). None of the antibodies reliably showed the nuclear BRCA1 staining anticipated from the other cell types. The absence of BRCA1 staining may be used as an indication of a lower concentration of BRCA1 in these nuclei and demonstrates the diversity of cross reactivities of these antibodies.

Cell cycle related nuclear distribution of BRCA1. We asked whether the appearance of disparate BRCA1 distributions might be due to changes in the cell cycle as previously reported (4, 10, 45). This was tested by comparing the BRCA1 distribution pattern with cell size and the distribution of centromeres. Centromeres are present in singles very early during the cell cycle, aggregate in late G1- and S-phases and can be found in doublets after the late S-phase replication of satellite DNA (for ref., see 46). Very early G1-phase cells remain connected and show the Fleming body, and as shown in Figure 4I, these daughter cells have no discreet BRCA1 domains. In contrast, the larger daughter cells have distinct BRCA1 accumulation and contain aggregated centromeres, suggestive of an S-phase cell. Late G1-phase cells have started to spread out on the glass surface but retain the single centromere distribution and with it, dispersed BRCA1 distribution (Figure 4J; top). Again, the larger cell pair in the same figure has BRCA1 accumulations and aggregated centromeres.

Large cell pairs with double centromers are considered cells in G2-phase of the cell cycle, and they largely have no BRCA1 accumulations (Figure 4K). We have, however, found large cells with a considerable amount of highly aggregated BRCA1. Most of these cells may be polyploid; i.e. going through nuclear cycles of replication without cytokinesis. The changes in BRCA1 distribution correlate with cell size and centromere distribution and are therefore cell cycle dependent.

Correlation of BRCA1 localization with other nuclear structures. Since the nucleus appears to be highly compartmentalized, we tested whether BRCA1 accumulations might co-localize with any of the known nuclear compartments. Triple labeling was used to observe the relative location of BRCA1 with the SC35 and ND10 domains. We found that BRCA1 accumulations are largely excluded from the SC35 domains and ND10 (Figure 5A). In this context, it is remarkable that ND10 are to a large extend situated adjacent to the SC35 domain, where as only a small fraction of the BRCA1 accumulations abut any of these structures. It is likely that those that do are fortuitously abutting without any functional significance.

The nuclear domain HP1a (31)has been reported to be cell cycle related in its distribution (47). When cells were double labeled for BRCA1 and HP1a, we found three distribution patterns as illustrated in adjacent cells in Figure 5B. In the middle and smallest cell, sizable accumulations of HP1a, but not BRCA1, are seen. The cell to the right shows several BRCA1 and HP1a accumulations that are mostly separated. However in the cell nucleus to the left, both antigens seem to be largely overlapping. This finding suggests that BRCA1 overlaps (colocalizes with) HP1a only in a specific part of the cell cycle, most probably during S-phase.

Since we had observed only very few cells with BRCA1 accumulations juxtaposed to ND10 and that these accumulations were usually rather large, we asked whether we could force more to this nuclear structure through the overexpression of BRCA1. When cells were transfected with the BRCA1 cDNA transcribed by the CMV promoter and probed 16 hrs. post transfection, we found all of the very large BRCA1 accumulations in close association with ND10 (Figure 5C). These BRCA1 aggregations had a near circular outline contrary to the more irregular outline of the endogenous large BRCA1 accumulations we occasionally found (Figure 5D; the nucleus is outlined in blue by staining for DNA). High BRCA1 aggregations are therefore associated with a specific nuclear domain, ND10. Surprisingly, large amounts of endogenous, as well as overexpressed, BRCA1 accumulated only at a limited number of ND10 and was not equally divided among the ND10 as expected for a protein transported into the nucleus through randomly positioned pore complexes. Therefore, we tested several proteins (that had been reported to associate with ND10) as to whether they where present at only a limited number of ND10 and whether they might be attracting the excess BRCA1. The herpesvirus ubiquitin specific protein (HAUSP) was the only protein that showed a limited association with ND10 (Figure 5E). Further, its distribution and accumulation did not overlap with that of BRCA1 (data not shown).

Effect of virus infection on the BRCA1 distribution. HAUSP has been characterized through its binding to the herpes virus (HSV1) immediate early protein ICP0. Since we could not find a direct binding of HAUSP with BRCA1, we asked whether the herpes virus immediate early protein ICP0, a transactivator that binds to HAUSP and disperses it from its

high accumulations at some ND10, would also disperse the high accumulations of BRCA1 from ND10. We infected cells with wild-type HSV1 for two hours. All infected cells could be identified by antibodies to the viral protein ICP0 and those so identified had only dispersed BRCA1 throughout the nucleus. Uninfected cells showed the expected BRCA1 accumulations (Figure 5F). This finding only shows that wild-type HSV1 infection disperses BRCA1 accumulations but provides the assay with which to test whether mutations in ICP0 would retain BRCA1 accumulations. When cells were infected with an ICP0 mutant, FXE (where the RING finger region has been deleted), BRCA1 accumulations were retained. This dispersion of BRCA1 in S-phase represents a new effect of the viral transactivator ICP0 on a host protein.

Adenovirus 5 (Ad5) also contains a protein (E4 ORF3) which modifies the location of HAUSP and ND10-associated proteins (39-41). We tested this virus early effect on BRCA1 distribution using the breast cancer cell line HBL100. In uninfected cells BRCA1 and ND10 are largely positioned in separate domains (Figure 5H).   However, three hours after infection, ND10 proteins were redistributed into many short tracks, and BRCA1 was now found in association with these tracks (Figure 5I). Previously we had shown by in situ hybridization that Ad5 replicates at sites where the viral single stranded DNA protein, DBP, accumulates (41). At these later stages (8 h.p.i.) we found BRCA1 juxtaposed to replication domains (Figure 5J). When these Ad5 replication domains expand, BRCA1 was recruited to these domains and surrounded them (Figure 5K). When viral replication advanced further, as indicated by the accumulation of DBP throughout much of the nucleus, BRCA1 is no longer detected around these sites, but only in those nuclear spaces where no viral accumulation is evident (left lower cell in Figure 5K). Finding BRCA1 to be recruited to the outside of the viral replication domain where transcription of this virus takes place, suggests that the virus makes use of this cellular protein in its transcriptional processes.

To test this hypothesis, we disturbed the global transcriptional processes through stress, which acts by shutting down normal transcription or processing and activating the transcription of the heat shock proteins (48-51). Such a global change may then either change BRCA1 distribution to: 1) a dispersed state in all cells, or 2) an accumulated state in all cells. When we treated HEp-2 cells for 1 h at 42° C, all BRCA1 accumulations were dispersed, with the BRCA1 distribution appearing as in cells in the G1-phase of the cell cycle. BRCA1 distribution therefore changes in response to stress (heat shock) as well as to DNA-damaging agents (10, 52).

10

Investigations of BRCA1's molecular interactions are progressing at several fronts but knowledge of supramolecular events involving BRCA1 is completely absent. In this report we have, therefore, begun to evaluate the distribution of BRCA1 at the cellular level during the cell cycle, determined its potential interactions at various nuclear domains and have started to define its behavior in response to external stimuli such as stress and viral infection. To embark on this work required antibodies that could be relied upon to visualize the location of BRCA1. Previously, BRCA1 had been shown to localize to the cell membrane and was considered a secreted protein (12). This localization has since been shown to be due to the cross reactivity of the C20 antibody to the EGF-receptor (52, 53). We therefore produced a monoclonal antibody (BR64) which recognizes the native antigen as well as BRCA1 expressed after transfection of various expression plasmids. When compared with other anti-BRCA1 MAbs, the MAb BR64 showed equivalent nuclear distribution, but also reacted with a cytoplasmic component, the centrosome. The same reactivity was found for other BRCA1 MAbs and the polyclonal antibody C20. Although the centrosome reactivity of all these antibodies may be a cross reactivity, the fact that the antibodies were made against quite different epitopes argues against this interpretation. We therefore consider that this result is suggestive of BRCA1 binding to this cellular domain so intimately involved in mitotic events. Furthermore, our use of BR64 hybridoma supernatant excludes the possibility of a contaminating mouse autoantibody. The reaction of C-20 with the Flemming body however, may be such an auto-antibody present in rabbits. The least useful monoclonal antibody for our analyses was 17F8, as it cross-reacted with a number of cytoplasmic granules. Furthermore, because of the thickness of the optical section, these granules overlaid the nuclear domain and did not allow for an unbiased determination of the nuclear distribution of BRCA1. The cross-reactivity of M13 with cytoplasmic filaments made this antibody useful only for cells without these filaments. We had observed, however, that even HEp-2 cells in mitosis had the cytoplasmic dot characteristic of depolymerized intermediate filaments. The faint cytoplasmic staining in HEp-2 cells may therefore be due to a low level of these filaments. The general conclusions of the comparison of the different BRCA1 antibodies is that 1) they collectively validate the presence of BRCA1 in the nucleus and 2) they can be used to evaluate the redistribution of BRCA1 induced by internal physiological changes and externally induced effects, but only in cells where the cross reactive proteins are absent.

For all antibodies, we had observed two distribution patterns for BRCA1 - dispersed and aggregated. That smaller cells had only dispersed BRCA1 suggested a cell cycle related event. A general interruption of the cell cycle is possible through the application of stress in the form of heat shock. Transcription and splicing is reduced and shifted to heat shock protein transcription. Under these conditions, BRCA1 becomes dispersed from its domains, similar to other proteins resident in other domains. Whether this phenomenon can be attributed to a change in transcription or to the subsequent cell cycle retardation, is not clear, but it presents a new single cell assay of an as-yet-to-be defined BRCA1 function.

There are no precise cell cycle markers that can be used in a single cell assay such as microscopy, particularly since the BRCA1 epitopes seem to be sensitive to the acid treatment necessary to expose the S-phase indicator BrdU (G. Maul, unpubl. results). However, He and Brinkley (46) showed that centromeres behave quite predictably during the cell cycle. The dispersion of the centromeres after mitosis lasts into later parts of G1-phase and was correlated with dispersed states of BRCA1. The centromeres aggregated later and the numbers that can be counted are far below those expected for the number of chromosomes

11

present. This stage corresponds, according to He and Brinkley (46), to the S-phase and is clearly correlated with the presence of aggregated BRCA1.   At the end of the cell cycle, cells are rather large and the centromeres are present as pairs and not highly clustered. The distribution pattern of BRCA1 in large cells is less clear but the bulk of those observed (which had paired centromeres) also had few or no sites of aggregated BRCA1. From these observations it is clear that BRCA1 changes its distribution during the cell cycle and that aggregation is predominantly present during the S-phase of the cell cycle with a more precise definition of this phenomenon not presently possible. Arising from these observations is the question of whether the areas of accumulation define the sites of active BRCA1, or whether, alternatively, BRCA1 may act in the "dispersed" mode with the "aggregated" state being sites of storage for BRCA1 (segregation).

The nucleus is partitioned into domains of various activities. Not only do specific chromosomal territories exist (54), but so do various extrachromosomal domains to which specific functions are attributable and which can be delineated with the respective antibodies. We did not find any domain that consistently colocalized with BRCA1. BRCA1 accumulations definitely reside outside of the SC35 domain and the ND10. However, BRCA1 accumulations overlap HP1a during a stage of S-phase. PIKA represent domains of highly aggregated HP1a, a protein that is normally associated with heterochromatin (47). HP1a has also been shown to change its aggregation pattern during the S-phase of the cell cycle (47).   Contrary to BRCA1, however, it starts in a highly aggregated, BRCA1 sized domains, during the G1-phase. The temporary association of the two proteins in the same nuclear domain does not necessarily signify direct interaction, a conclusion supported by a two hybrid assay in which no interaction could be found (unpubl. results).   Other proteins may be intermediaries; However, these two proteins are the only ones presently showing cell cycle-dependent co-localization.

The accumulation of a protein may be viewed as indicative of 1) functioning at this site, or 2) as segregation with the implication of removing the protein from functioning, or 3) storing excess protein as a means to regulate the precise amount of protein in a delicate balance. This balance may change during the cell cycle. Under these assumptions we may either conclude that BRCA1 has specific nuclear sites of high activity during S-phase or its concentration throughout the nucleus is lowered by segregation during this part of the cell cycle.   The possibility that the cell has the capability to segregate endogenous BRCA1 is supported by the finding of high concentrations close to ND10 and the accumulation of BRCA1 at these sites when overexpressed.   We may be witnessing segregation of BRCA1 into a nuclear dump or nuclear depot (55).

Viruses have often been instrumental in the elucidation of cellular functions. Using two DNA viruses we could demonstrate that they modify BRCA1 distribution quite differently and provide a single cell assay to test this perturbation. The dispersion of BRCA1 by Herpes Simplex Virus type 1 (HSV1) may be due to the interruption of the cell cycle as HSV1 blocks S-phase (56). However, we were able to define the immediate early HSV1 IE1 gene as an essential gene for BRCA1 dispersion.   Its potential interaction with a BRCA1 pathway may lay at the center of the inability of cells to grow when ICP0 is constituitivly expressed (G. Maul, unpublished results).

Adenovirus 5 has a quite different effect on BRCA1. BRCA1 accumulates at and surrounds some of the replication sites during the viral replication.   Later, after transcription and replication cease late in the replication cycle, BRCA1 is no longer present around the

12

viral replication domain as indicated by staining against DBP.   The outer fringe of the replication site represents viral single-stranded DNA that is being transcribed, whereas the center contains double stranded Ad5 DNA (57).   The presence of BRCA1 at the outer region of Ad5 suggests that it may be utilized in viral transcription.   Alternatively, since this outer region is also where decatenation of the viral DNA takes place, BRCA1 accumulation in this area may suggest a role in this process, a role supported by the observation that BRCA1 is involved in the crossover mechanism during pachyteen of meiosis (9).

This investigation establishes that there is a cell cycle related change in the distribution of BRCA1 in the nucleus and that another protein, HP-1, involved in transcriptionally silencing of chromatin, colocalizes during part of BRCA1 accumulation/segregation. We find that DNA viruses change the distribution of BRCA1 substantially and, in the case of Ad5, temporarily recruit this protein into an area of high transcriptional activity.

Conclusions

We generated a new monoclonal antibody and compared it with other anti-BRCA1 antibodies. The general conclusions derived from the comparison of the different BRCA1 antibodies is that 1) they collectively validate the presence of BRCA1 in the nucleus and 2) they can be used to evaluate the redistribution of BRCA1 induced by physiological changes, but only in cells where cross-reactive proteins are absent.

1. In our analysis of BRCA1 sub-nuclear localization, we observed two distribution patterns - dispersed and aggregated. That smaller cells had only dispersed BRCA1 suggested a cell cycle related event. In order to test a possible cell-cycle related "movement" of BRCA1, we employed a general interruption of the cell cycle through the application heat shock. Under these conditions the cell cycle is interupted ("blocked") and other proteins, resident in other domains, become dispersed from these domains. Application of heat shock caused BRCA1 to become dispersed, similar to that seen for other "domain" proteins. Whether this phenomenon can be attributed to a change in gene transcription or to the subsequent cell cycle retardation is not clear, but it presents a new single cell assay of an as-yet-to-be defined BRCA1 function.

2. In our attempts to co-localize BRCA1 to the same sub-nuclear domains as other proteins (eg. PML, SC35, HP1a), we did not find any domain/protein that consistently co-localized with BRCA1. BRCA1 "domains" definitely reside outside of RNA splicing domains (SC35) and the ND10 domains (PML). However, BRCA1 accumulations overlapped with accumulations of HP1a during a stage of S-phase.   HP1a, a protein that is normally associated with heterochromatin, has also been shown to change its aggregation pattern during the S-phase of the cell cycle. However, contrary to BRCA1, it starts in a highly aggregated state during the G1-phase and then becomes dispersed during the S-phase of the cell cycle. Though intriguing, the temporary association of the two proteins in the same nuclear domain does not necessarily signify direct interaction.

2. Using two DNA viruses we could demonstrate that they modify BRCA1 distribution differently, suggesting that these viruses will be useful tools in determing a function for BRCA1. The Herpes Simplex Virus type 1 (HSV1) disperses BRCA1 from its aggregated domains. This may be due to the interruption of the cell cycle as HSV1 is known to block cells in S-phase (this result is similar to that obtained with heat shock). Furthermore, we were able to define the immediate early HSV1 IE1 gene as an essential gene for this BRCA1 dispersion. Adenovirus 5 (Ad5) has a quite different effect on BRCA1. After infection with Ad5, BRCA1 accumulated at, and surrounded some of, the Ad5 viral replication sites. The outer fringe of the replication site represents viral single-stranded DNA that is being transcribed, whereas the center contains double-stranded Ad5 DNA. The presense of BRCA1 at the outer region of Ad5 suggests that it may be utilized in viral transcription. If confirmed, this would provide further evidence of a role for BRCA1 in cellular transcription. Alternatively, since this outer region is also where decatenation of the viral DNA takes place (unlinking of circular DNA), BRCA1 accumulation in this area may suggest a role in this process, a role supported by the observation that BRCA1 is involved in the crossover mechanism during pachyteen of meiosis.

We are currently revising a manuscript containing the above conclusions.

References

1. Miki, Y., Swensen, J., Shattuck-Eidens, D., Futreal, P. A., Harshman, K., Tavtigian, S., Liu, Q., Cochran, C., Bennett, L. M., Ding, W. and et al. A strong candidate for the breast and ovarian cancer susceptibility gene BRCA1. Science, *266:* 66-71, 1994.
2. Chen, C. F., Li, S., Chen, Y., Chen, P. L., Sharp, Z. D. and Lee, W. H. The nuclear localization sequences of the BRCA1 protein interact with the importin-alpha subunit of the nuclear transport signal receptor. Journal of Biological Chemistry, *271:* 32863-32868, 1996.
3. Wu, L. C., Wang, Z. W., Tsan, J. T., Spillman, M. A., Phung, A., Xu, X. L., Yang, M. C., Hwang, L. Y., Bowcock, A. M. and Baer, R. Identification of a RING protein that can interact in vivo with the BRCA1 gene product. Nature Genetics, *14:* 430-440, 1996.
4. Jin, Y., Xu, X. L., Yang, M.-C. W., Wei, F., Ayi, T.-C., Bowcock, A. M. and Baer, R. Cell cycle-dependent colocalization of BARD1 and BRCA1 proteins in discrete nuclear domains. Proc. Natl. Acad. Sci., USA, *94:* 12075-12080, 1997.
5. Jensen, D. E., Proctor, M., Marquis, S. T., Gardner, H. P., Ha, S. I., Chodosh, L. A., Ishov, A. M., Tommerup, N., Vissing, H., Sekido, Y., Minna, J., Borodovsky, A., Schultz, D. C., Wilkinson, K. D., Maul, G. G., Barlev, N., Berger, S. L., Prendergast, G. C. and Rauscher, F. J., 3rd BAP1: a novel ubiquitin hydrolase which binds to the BRCA1 RING finger and enhances BRCA1-mediated cell growth suppression. Oncogene, *16:* 1097-1112, 1998.
6. Thompson, M. E., Jensen, R. A., Obermiller, P. S., Page, D. L. and Holt, J. T. Decreased expression of BRCA1 accelerates growth and is often present during sporadic breast cancer progression. Nat Genet, *9:* 444-450, 1995.
7. Rao, V. N., Shao, N., Ahmak, M. and Reddy, E. S. P. Antisense RNA to the putative tumor suppressor gene BRCA1 transforms mouse fibroblasts. Oncogene, *12:* 523-528, 1996.

8. Holt, J. T., Thompson, M. E., Szabo, C., Robinson-Benion, C., Arteaga, C. L., King, M.-C. and Jensen, R. A. Growth retardation and tumour inhibition by BRCA1. Nature Genetics, *12:* 298-302, 1996.

9. Scully, R., Chen, J., Plug, A., Xiao, Y., Weaver, D., Feunteun, J., Ashley, T. and Livingston, D. M. Association of BRCA1 with Rad51 in mitotic and meiotic cells. Cell, *88:* 265-275, 1997.

10. Scully, R., Chen, J., Ochs, R. L., Keegan, K., Hoekstra, M., Feunteun, J. and Livingston, D. M. Dynamic changes of BRCA1 subnuclear location and phosphorylation state are initiated by DNA damage. Cell, *90:* 425-435, 1997.

11. Chen, Y., Chen, C. F., Riley, D. J., Allred, D. C., Chen, P. L., Von Hoff, D., Osborne, C. K. and Lee, W. H. Aberrant subcellular localization of BRCA1 in breast cancer. Science, *270:* 789-791, 1995.

12. Jensen, R. A., Thompson, M. E., Jetton, T. L., Szabo, C. I., van der Meer, R., Helou, B., Tronick, S. R., Page, D. L., King, M.-C. and Holt, J. T. BRCA1 is secreted and exhibits properties of a granin. Nature Genetics, *12:* 303-308, 1996.

13. Koonin, E. V., Altschul, S. F. and Bork, P. BRCA1 protein products: ...functional motifs... Nature Genet., *13:* 266-268, 1996.

14. Chapman, M. S. and Verma, I. M. Transcriptional activation by BRCA1 [letter; comment]. Nature, *382:* 678-679, 1996.

15. Scully, R., Anderson, S. F., Chao, D. M., Wei, W., Ye, L., Young, R. A., Livingston, D. M. and Parvin, J. D. BRCA1 is a component of the RNA polymerase II holoenzyme. Proceedings of the National Academy of Sciences of the United States of America, *94:* 5605-5610, 1997.

16. Borden, K. L., Boddy, M. N., Lally, J., O'Reilly, N. J., Martin, S., Howe, K., Solomon, E. and Freemont, P. S. The solution structure of the RING finger domain from the acute promyelocytic leukaemia proto-oncoprotein PML. Embo J, *14:* 1532-1541, 1995.

17. Lovering, R., Hanson, I. M., Borden, K. L., Martin, S., O'Reilly, N. J., Evan, G. I., Rahman, D., Pappin, D. J., Trowsdale, J. and Freemont, P. S. Identification and preliminary characterization of a protein motif related to the zinc finger. Proc Natl Acad Sci U S A, *90:* 2112-2116, 1993.

18. Klug, A. and Schwabe, J. W. Protein motifs 5. Zinc fingers. FASEB Journal, *9:* 597-604, 1995.

19. Saurin, A. J., Borden, K. L. B., Boddy, M. N. and Freemont, P. S. Does this have a familiar RING? Trends in Biochem. Sci., *21:* 208-214, 1996.

20. Friedman, J. R., Fredericks, W. J., Jensen, D. E., Speicher, D. W., Huang, X. P., Neilson, E. G. and Rauscher, F. J. r. KAP-1, a novel corepressor for the highly conserved KRAB repression domain. Genes & Development, *10:* 2067-2078, 1996.

21. Gudas, J. M., Nguyen, H., Li, T. and Cowan, K. H. Hormone-dependent regulation of BRCA1 in human breast cancer cells. Cancer Res, *55:* 4561-4565, 1995.

22. Gudas, J. M., Tao, L., Nguyen, H., Jensen, D., Rauscher III, F. J. and Cowan, K. H. Cell Cycle Regulation of BRCA1 Messenger RNA in Human Breast Epithelial Cells. Cell Growth and Differentiation, *7:* 717-723, 1996.

23. Vaughn, J. P., Davis, P. L., Jarboe, M. D., Huper, G., Evans, A. C., Wiseman, R. W., Berchuck, A., Iglehart, J. D., Futreal, A. and Marks, J. R. BRCA1 expression is induced before DNA synthesis in both normal and tumor-derived breast cells. Cell Growth and Differentiation, *7:* 711-715, 1996.

24. Marks, J. R., Huper, G., Vaughn, J. P., Davis, P. L., Norris, J., McDonnell, D. P., Wiseman, R. W., Futreal, P. A. and Iglehart, J. D. BRCA1 expression is not directly responsive to estrogen. Oncogene, *14:* 115-121, 1997.

25. Fu, X. D. and Maniatis, T. Factor required for mammalian spliceosome assembly is localized to discrete regions in the nucleus. Nature, *343:* 437-441, 1990.

26. Spector, D. L., Fu, X. D. and Maniatis, T. Associations between distinct pre-mRNA splicing components and the cell nucleus. EMBO Journal, *10:* 3467-3481, 1991.

27. Carmo-Fonseca, M., Pepperkok, R., Carvalho, M. T. and Lamond, A. I. Transcription-dependent colocalization of the U1, U2, U4/U6, and U5 snRNPs in coiled bodies. Journal of Cell Biology, *117:* 1-14, 1992.

28. Frey, M. R. and Matera, A. G. Coiled bodies contain U7 small nuclear RNA and associate with specific DNA sequences in interphase human cells [published erratum appears in Proc Natl Acad Sci U S A 1995 Aug 29;92(18):8532]. Proceedings of the National Academy of Sciences of the United States of America, *92:* 5915-5919, 1995.

29. Smith, K. P., Carter, K. C., Johnson, C. V. and Lawrence, J. B. U2 and U1 snRNA gene loci associate with coiled bodies. Journal of Cellular Biochemistry, *59:* 473-485, 1995.

30. Gao, L., Frey, M. R. and Matera, A. G. Human genes encoding U3 snRNA associate with coiled bodies in interphase cells and are clustered on chromosome 17p11.2 in a complex inverted repeat structure. Nucleic Acids Research, *25:* 4740-4747, 1997.

31. Saunders, W. S., Cooke, C. A. and Earnshaw, W. C. Compartmentalization within the nucleus: discovery of a novel subnuclear region. Journal of Cell Biology, *115:* 919-931, 1991.

32. Dyck, J. A., Maul, G. G., Miller, W. H., Jr., Chen, J. D., Kakizuka, A. and Evans, R. M. A novel macromolecular structure is a target of the promyelocyte-retinoic acid receptor oncoprotein. Cell, *76:* 333-343, 1994.

33. Desbois, C., Rousset, R., Bantignies, F. and Jalinot, P. Exclusion of Int-6 from PML nuclear bodies by binding to the HTLV-I Tax oncoprotein. Science, *273:* 951-953, 1996.

34. Maul, G. G., Ishov, A. M. and Everett, R. D. Nuclear domain 10 as preexisting potential replication start sites of herpes simplex virus type-1. Virology, *217:* 67-75, 1996.

35. Ishov, A. M., Stenberg, R. M. and Maul, G. G. Human cytomegalovirus immediate early interaction with host nuclear structures: definition of an immediate transcript environment. Journal of Cell Biology, *138:* 5-16, 1997.

36. Maul, G. G., Guldner, H. H. and Spivack, J. G. Modification of discrete nuclear domains induced by herpes simplex virus type 1 immediate early gene 1 product (ICP0). Journal of General Virology, *74:* 2679-2690, 1993.

37. Maul, G. G. and Everett, R. D. The nuclear location of PML, a cellular member of the C3HC4 zinc-binding domain protein family, is rearranged during herpes simplex virus infection by the C3HC4 viral protein ICP0. Journal of General Virology, *75:* 1223-1233, 1994.

38. Everett, R. D. and Maul, G. G. HSV-1 IE protein Vmw110 causes redistribution of PML. EMBO Journal, *13:* 5062-5069, 1994.

39. Carvalho, T., Seeler, J. S., Ohman, K., Jordan, P., Pettersson, U., Akusjarvi, G., Carmo-Fonseca, M. and Dejean, A. Targeting of adenovirus E1A and E4-ORF3 proteins to nuclear matrix-associated PML bodies. Journal of Cell Biology, *131:* 45-56, 1995.

40. Doucas, V., Ishov, A. M., Romo, A., Juguilon, H., Weitzman, M. D., Evans, R. M. and Maul, G. G. Adenovirus replication is coupled with the dynamic properties of the PML nuclear structure. Genes & Development, *10:* 196-207, 1996.

41. Ishov, A. M. and Maul, G. G. The periphery of nuclear domain 10 (ND10) as site of DNA virus deposition. Journal of Cell Biology, *134:* 815-826, 1996.

42. Thakur, S., Zhang, H. B., Peng, Y., Le, H., Carroll, B., Ward, T., Yao, J., Farid, L. M., Couch, F. J., Wilson, R. B. and Weber, B. L. Localization of BRCA1 and a splice variant identifies the nuclear localization signal. Molecular & Cellular Biology, *17:* 444-452, 1997.

43. Hogervorst, F. B., Cornelis, R. S., Bout, M., van Vliet, M., Oosterwijk, J. C., Olmer, R., Bakker, B., Klijn, J. G., Vasen, H. F., Meijers-Heijboer, H. and et al. Rapid detection of BRCA1 mutations by the protein truncation test. Nat Genet, *10:* 208-212, 1995.

44. Patarca, R., Freeman, G. J., Schwartz, J., Singh, R. P., Kong, Q. T., Murphy, E., Anderson, Y., Sheng, F. Y., Singh, P., Johnson, K. A. and et al. rpt-1, an intracellular protein from helper/inducer T cells that regulates gene expression of interleukin 2 receptor and human immunodeficiency virus type 1. Proc Natl Acad Sci U S A, *85:* 2733-2737, 1988.

45. Chen, Y., Farmer, A. A., Chen, C. F., Jones, D. C., Chen, P. L. and Lee, W. H. BRCA1 is a 220-kDa nuclear phosphoprotein that is expressed and phosphorylated in a cell cycle-dependent manner. Cancer Research, *56:* 3168-3172, 1996.

46. He, D. and Brinkley, B. R. Structure and dynamic organization of centromeres/prekinetochores in the nucleus of mammalian cells. Journal of Cell Science, *109:* 2693-2704, 1996.

47. Saunders, W. S., Chue, C., Goebl, M., Craig, C., Clark, R. F., Powers, J. A., Eissenberg, J. C., Elgin, S. C., Rothfield, N. F. and Earnshaw, W. C. Molecular cloning of a human homologue of Drosophila heterochromatin protein HP1 using anti-centromere autoantibodies with anti-chromo specificity. Journal of Cell Science, *104:* 573-582, 1993.

48. Sadis, S., Hickey, E. and Weber, L. A. Effect of heat shock on RNA metabolism in HeLa cells. Journal of Cellular Physiology, *135:* 377-386, 1988.

49. Utans, U., Behrens, S. E., Luhrmann, R., Kole, R. and Kramer, A. A splicing factor that is inactivated during in vivo heat shock is functionally equivalent to the [U4/U6.U5] triple snRNP-specific proteins. Genes & Development, *6:* 631-641, 1992.

50. Bond, U. Heat shock but not other stress inducers leads to the disruption of a sub-set of snRNPs and inhibition of in vitro splicing in HeLa cells [published erratum appears in EMBO J 1988 Dec 1;7(12):4020]. EMBO Journal, *7:* 3509-3518, 1988.

51. Yost, H. J. and Lindquist, S. RNA splicing is interrupted by heat shock and is rescued by heat shock protein synthesis. Cell, *45:* 185-193, 1986.

52. Thomas, J. E., Smith, M., Rubinfeld, B., Gutowski, M., Beckmann, R. P. and Polakis, P. Subcellular localization and analysis of apparent 180-kDa and 220-kDa proteins of the breast cancer susceptibility gene, BRCA1. Journal of Biological Chemistry, *271:* 28630-28635, 1996.

53. Wilson, C., Payton, M. N., Pekar, S. K., Zhang, K., Pacifici, R. E., Gudas, J. L., Thukral, S., Calzone, F. J., Reese, D. M. and Slamon, D. I. BRCA1 protein products: Antibody Specificity... Nature Genet., *13:* 264-265, 1996.

54. Lichter, P., Cremer, T., Borden, J., Manuelidis, L. and Ward, D. C. Delineation of individual human chromosomes in metaphase and interphase cells by in situ suppression hybridization using recombinant DNA libraries. Human Genetics, *80:* 224-234, 1988.

55. Maul, G. G. Nuclear Domain 10, the site of DNA virus transcription and replication. BioEssay, *In Press:* 1998.

56. de Bruyn Kops, A. and Knipe, D. M. Formation of DNA replication structures in herpes virus-infected cells requires a viral DNA binding protein. Cell, *55:* 857-868, 1988.

57. Thiry, M. and Puvion-Dutilleul, F. Differential distribution of single-stranded DNA, double-stranded DNA, and RNA in adenovirus-induced intranuclear regions of HeLa cells. Journal of Histochemistry & Cytochemistry, *43:* 749-759, 1995.

58. Madden, S. L., Cook, D. M., Morris, J. F., Gashler, A., Sukhatme, V. P. and Rauscher, F. J., III Transcriptional repression mediated by the WT1 Wilms tumor gene product. Science, *253:* 1550-1553, 1991.

59. Chen, C. and Okayama, H. High-efficiency transformation of mammalian cells by plasmid DNA. Molecular & Cellular Biology, *7:* 2745-2752, 1987.

60. Scully, R., S., G., Brown, M., Caprio, J. A. D., Cannistra, S. A., Feunteun, J., Schnitt, S. and Livingston, D. M. Location of BRCA1 in human breast and ovarian cancer cells. Science, *272:* 123-126, 1996.

61. Maul, G. G., Yu, E., Ishov, A. M. and Epstein, A. L. Nuclear domain 10 (ND10) associated proteins are also present in nuclear bodies and redistribute to hundreds of nuclear sites after stress. Journal of Cellular Biochemistry, *59:* 498-513, 1995.

Appendices

I. Figure Legends and data figures
II. Published Manuscript

I.

Figure 1. (A) Diagrammatic representation of the BRCA1 protein and the RING finger domain used to generate the 6XHis-BRCA1-RF fusion protein. The identified fusion protein was produced in bacteria, purified by Ni-NTA chromotagraphy (Qiagen, Inc.), and analyzed by SDS-PAGE for purity. Shown is a photograph of the coomassie blue stained gel. (B). The amino-terminal 100 amino acids of human BRCA1 (including the RING finger domain) or the indicated amino acids of the various BRCA1-RF mutants, deletions and controls were fused to the LexA DNA-binding domain. These constructs were then used to produce the fusion protein by coupled *in vitro* transcription and translation. These proteins were used without further purification in immuno-precipitation analyses with the BR64 MAb. A summary of the results shown in Figure 2 is shown to the right of the diagrams.

Figure 2. (A) The BR64 mAb detects only the BRCA1 RING finger domain. The indicated RING finger-containing proteins were transcribed and translated *in vitro* in the presence of ^{35}S-methionine. They were then immunoprecipitated with the BR64 mAb and the bound proteins were separated by SDS-PAGE. Proteins were then detected by fluorography. (B) BRCA1 RING finger domains containing missense mutations can be detected by BR64. Mutations found in breast cancer kindreds were introduced into LexA-BRCA1-RF fusion proteins. These proteins were transcribed and translated *in vitro* in the presence of ^{35}S-methionine, followed by immunoprecipitation with the BR64 mAb. Bound proteins were separated by SDS-PAGE and detected by fluorography. LexA-RPT-1 is a fusion protein containing the RING finger domain from the RPT-1 protein. (C) Amino acids 80-100 of the BRCA1 protein contain the epitope for the BR64 mAb. Truncated LexA-BRCA1-RF fusion proteins were transcribed and translated *in vitro* in the presence of ^{35}S-methionine and then immunoprecipitated with the BR64 mAb. Bound proteins were detected by fluorography after separation by SDS-PAGE.
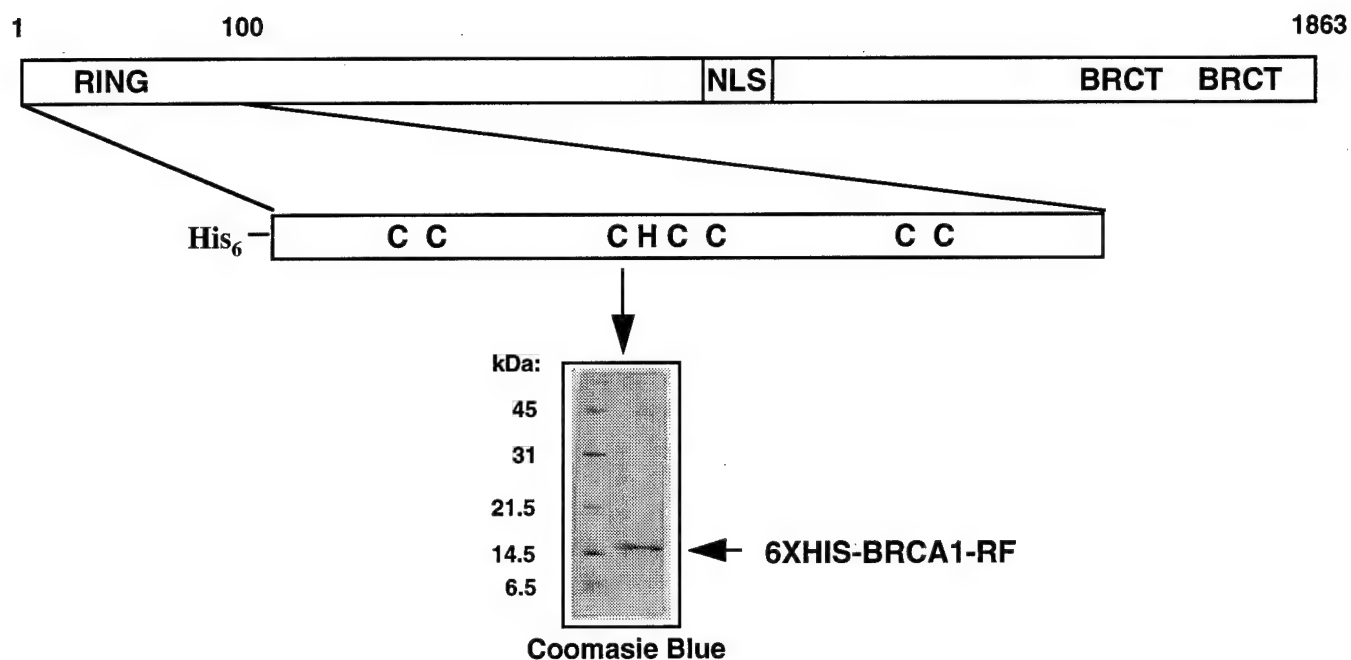
Figure 3. BR64 detects endogenous BRCA1 protein. (A) Whole cell extracts from ^{32}PO$_4$ -labeled MDA-468 breast cancer cells (5-7 X 10^6 cells) were immunoprecipitated with the BR64 mAb or the C-20 polyclonal Ab. A BRCA1 cDNA was transcribed and translated *in vitro* in the presence of ^{35}S-methionine to produce protein for size comparison purposes. Proteins were separated by SDS-PAGE and detected by fluorography. (B) Whole cell extracts from the breast cancer cell line HBL-100 (1-2 X10^6 cells) were immunoprecipitated with pre-immune sera or with anti-BRCA1-RF polyclonal antibodies. The immunoprecipitated proteins were separated by SDS-PAGE and transferred to a PVDF membrane. The membrane was immunoblotted with the BR64 mAb and detected with HRP-conjugated goat anti-mouse IgG. (C) Nuclear extract from HeLa cells was separated by SDS-PAGE and

transferred to a PVDF membrane. The membrane was immunoblotted with the BR64 mAb and detected with Alkaline Phosphatase-conjugated goat anti-mouse IgG.

Figure 4. Characterization of BRCA1 distribution in different cells and relative to different nuclear domains by immunofluorescence microscopy. The color is given for each of the different antigens in the upper corners of each individual image. **A**, MAb BR64 labeled HEp-2; arrows point to cytoplasmic double dots representing the centrosome. **B**, MAb M13 labeling HEp-2 cells. **C**, MAb 17F8 labeling HEp-2 cells. **D**, polyclonal antibody C-20 labeling HEp-2 cells. **E**, MAb BR64 labeling of MDA cells; arrows pointing to centrosome. **F**, MAb M13 labeling MDA cells showing dominant fibrillar cytoplasmic staining. **G**, Mab 17F8 labeling MDA cells showing strong staining of cytoplasmic granules. **H**, double labeling of HEp-2 cells using polyclonal antibody C-20 and BR64 showing complete overlap. **I**, double labeling of HEp-2 cells using MAb BR64 and human anti-centromere antibodies to show in the upper half daughter cells in early G1 phase and larger daughter cells with aggregated centromeres. **J**, same as I but showing G1-phase cell at a later time after mitosis and two larger cells with aggregated centromeres suggestive of S-phase cells. **K**, same staining as I having two large cells with centromeres which are often present as doublets suggestive of G2-phase cells.

Figure 5. BRCA1 distribution in relation to other nuclear domains and after virus infection. **A**, triple labeling of HBL100 cell showing BRCA1 staining not to co-localize with SC35 domains and ND10. **B**, double labeling of HBL100 cells showing that HP-1 may or may not co-localize with BRCA1. **C**, BRCA1 transfected HEp-2 cell showing that overexpressed BRCA1 localizes adjacent to a few ND10. **D**, HEp-2 cell showing high concentrations of endogenous BRCA1 at ND10. **E**, HEp-2 cell double labeled to show that HAUSP localizes adjacent to only a few ND10. **F,** HEp-2 cells 2 h p.i. with wt. type HSV-1. Cells are double labeled for ICP0 to show which cells are infected and BRCA1 demonstrating that BRCA1 is dispersed in infected cells. **G**, same as A, but infected with the RING finger mutant FXE of HSV-1 indicating that infection with this mutant does not disperse BRCA1. **H**, uninfected HBL100 cells showing the normal distribution of BRCA1 relative to ND10. **I**, HBL100 cells h p.i. with Ad5 and stained for BRCA1 and sp100 indicating that sp100 has been distributed to short tracks and BRCA1 is located at many of these tracks. **J**. HEp-2 cells 8 h p.i. with Ad5 and stained to show the single stranded DNA binding protein DBP as an indicator where Ad5 replication begins and demonstrating that BRCA1 localizes adjacent to the replication domains. **K**, HEp-2 cells 12 h p.i. with Ad5, double labeled for DBP and BRCA1, indicating that BRCA1 localizes to the outer rim of the replication compartment Upper right) and is absent from the replication compartment at later stages of the replication cycle (lower left). **L**, HBL100 cells stressed for 1 h at 42° C and labeled for BRCA1. All BRCA1 accumulations have dispersed.
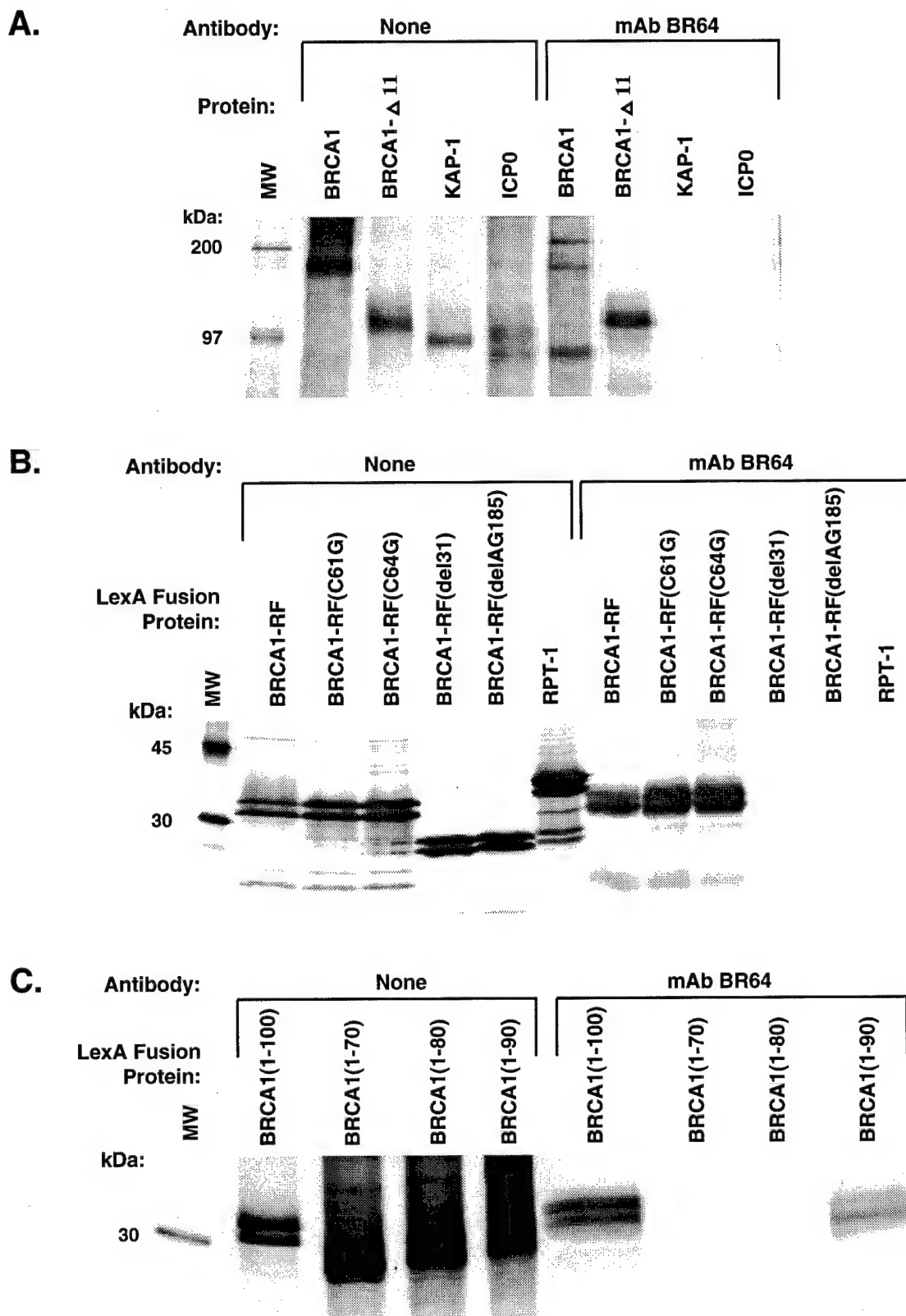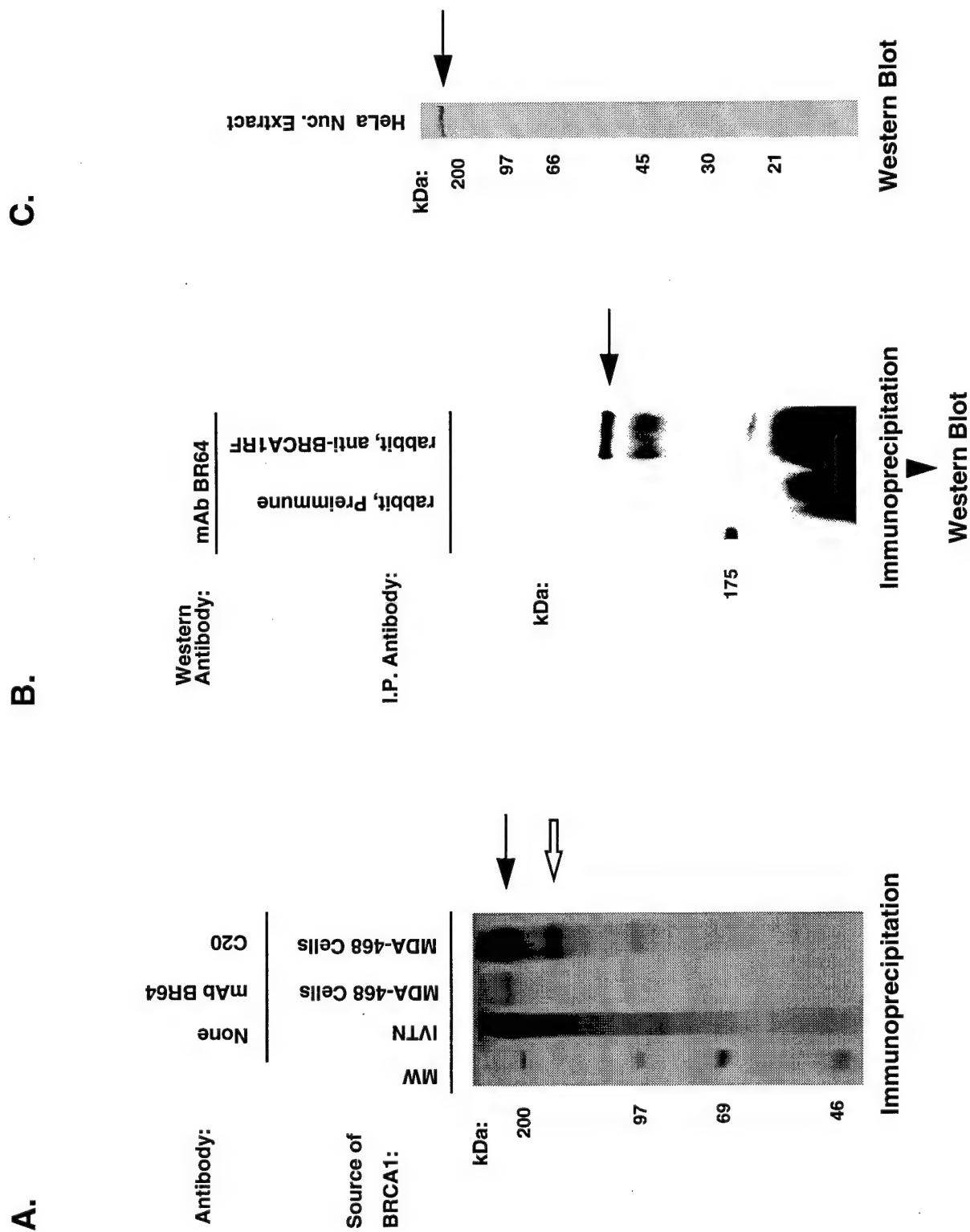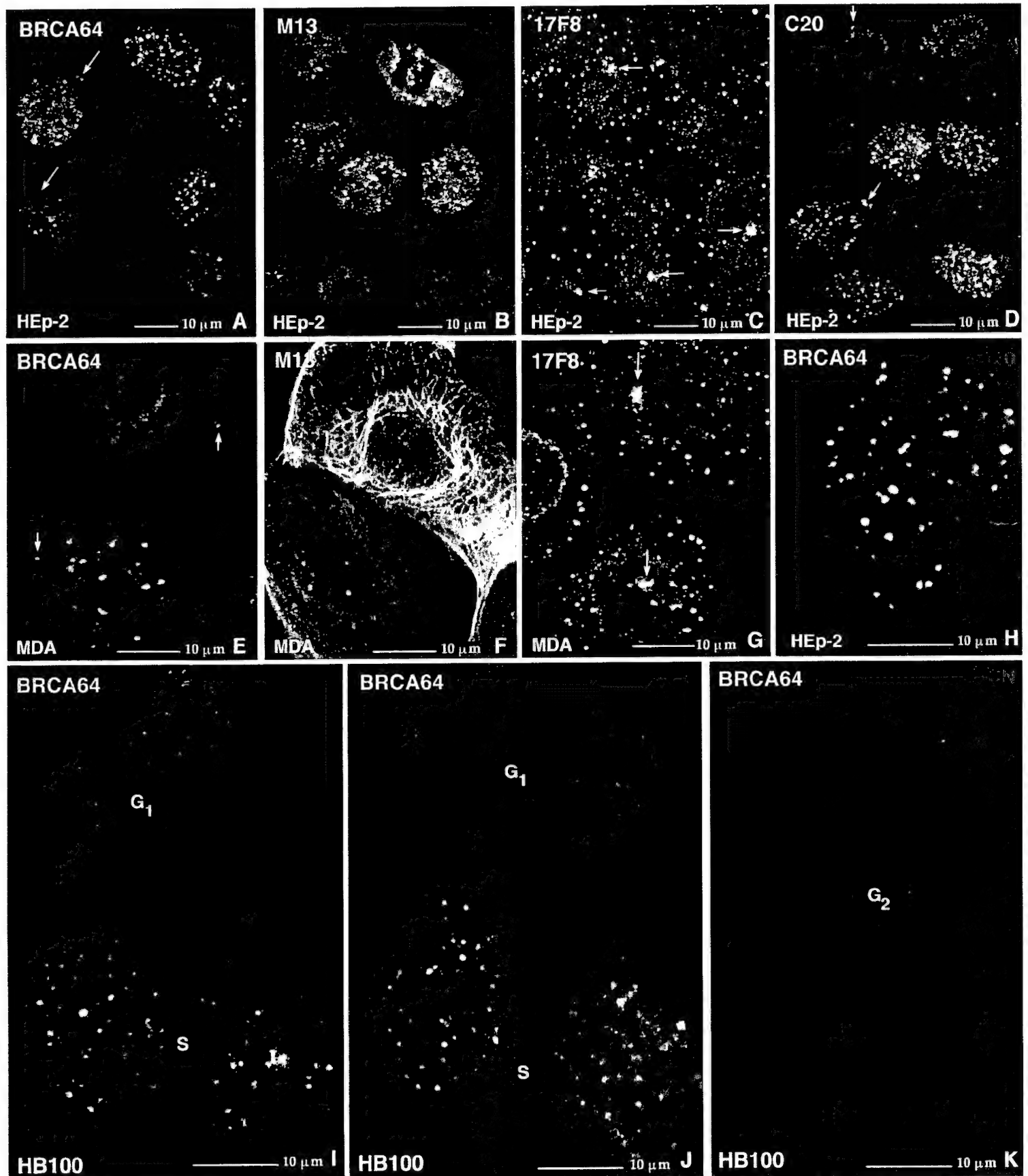
A.

B.

		MAb BR64 Interaction
BRCA1-RF	LexA ... CC CHCC CC (1-100)	++
BRCA1(1-90)	LexA ... CC CHCC CC (1-90)	+
BRCA1(1-80)	LexA ... CC CHCC CC (1-80)	−
BRCA1(1-70)	LexA ... CC CHCC CC (1-70)	−
BRCA1(C64G)-RF	LexA ... CC CHCC C[G] (1-100)	++
BRCA1(C61G)-RF	LexA ... CC CHCC [G]C (1-100)	++
BRCA1-delAG185	LexA ... (1-22-39)	−
BRCA1-del31	LexA ... CC (1-31-35)	−
RPT-1-RF	LexA ... CC CHCC CC (1-100)	−

Fig. 1

Fig. 2

Fig. 3

Fig. 4

Fig. 5

BAP1: a novel ubiquitin hydrolase which binds to the BRCA1 RING finger and enhances BRCA1-mediated cell growth suppression

David E Jensen[1], Monja Proctor[2], Sandra T Marquis[6], Heather Perry Gardner[6], Seung I Ha[6], Lewis A Chodosh[6], Alexander M Ishov[1], Niels Tommerup[3], Henrik Vissing[4], Yoshitaka Sekido[2], John Minna[2], Anna Borodovsky[5], David C Schultz[1], Keith D Wilkinson[5], Gerd G Maul[1], Nickolai Barlev[1], Shelley L Berger[1], George C Prendergast[1] and Frank J Rauscher III[1]

[1]The Wistar Institute, 3601 Spruce Street, Philadelphia, Pennsylvania 19104, USA; [2]Hamon Center for Therapeutic Oncology Research, University of Texas Southwestern Medical Center, Dallas, Texas 75235, USA; [3]John F. Kennedy Institute, 2600 Glostrup, Denmark and The Department of Medical Genetics, The Panum Institute, University of Copenhagen, DK2200 Copenhagen, Denmark; [4]Department of Molecular Genetics, Novo Nordisk, DK-2880 Bagsvaerd, Denmark; [5]Department of Biochemistry, Emory University, Atlanta, Georgia 30322, USA; [6]Department of Molecular and Cellular Engineering, University of Pennsylvania School of Medicine, Philadelphia, Pennsylvania 19104, USA

We have identified a novel protein, BAP1, which binds to the RING finger domain of the Breast/Ovarian Cancer Susceptibility Gene product, BRCA1. BAP1 is a nuclear-localized, ubiquitin carboxy-terminal hydrolase, suggesting that deubiquitinating enzymes may play a role in BRCA1 function. BAP1 binds to the wild-type BRCA1-RING finger, but not to germline mutants of the BRCA1-RING finger found in breast cancer kindreds. BAP1 and BRCA1 are temporally and spatially co-expressed during murine breast development and remodeling, and show overlapping patterns of subnuclear distribution. BAP1 resides on human chromosome 3p21.3; intragenic homozgyous rearrangements and deletions of BAP1 have been found in lung carcinoma cell lines. BAP1 enhances BRCA1-mediated inhibition of breast cancer cell growth and is the first nuclear-localized ubiquitin carboxy-terminal hydrolase to be identified. BAP1 may be a new tumor suppressor gene which functions in the BRCA1 growth control pathway.

Keywords: ubiquitin hydrolase; BRCA1; chromosome 3p21.3; RING finger

Introduction

The cloning of the chromosome 17q21 BRCA1 breast cancer susceptibility gene is a landmark accomplishment in cancer genetics (Miki et al., 1994). Germline mutations in BRCA1 appear to account for ~50% of familial breast cancers and essentially all families with 17q21-linked inherited susceptibility to ovarian and breast cancer (Szabo and King, 1995). The importance of this gene is underscored by the fact that kindreds segregating constitutional BRCA1 mutations show a lifetime risk of 40–50% for ovarian cancer and >80% for breast cancer (Easton et al., 1993, 1995). The classification of BRCA1 as a highly penetrant, autosomal dominant tumor suppressor gene has been genetically confirmed by the finding of frequent LOH of the wild-type allele in breast tumors from mutation

carriers (Hall et al., 1990; Miki et al., 1994; Smith et al., 1992). Surprisingly, BRCA1 mutations in sporadic breast cancer, including those which show 17 g LOH, have yet to be found and BRCA1 mutations are extremely rare in sporadic ovarian cancer (Futreal et al., 1994; Merajver et al., 1995).

The BRCA1 locus spans >100 kb comprising 24 exons (Miki et al., 1994). More than 100 constitutional mutations have been identified in BRCA1 over the entire length of the gene. Some clustering of these mutations has been seen in populations, and genotype-phenotype correlations have been suggested (FitzGerald et al., 1996; Ford et al., 1994; Muto et al., 1996; Roa et al., 1996; Struewing et al., 1995). The majority of germline mutations result in a truncated BRCA1 protein although recurrent missense mutations resulting in amino acid substitutions in kindreds have also been observed (Couch and Weber, 1996). The heterogeneity of BRCA1 mutant proteins produced by this spectrum of genetic mutations suggests that multiple, independent functions and/or protein–protein interaction surfaces are targets for mutational inactivation. However, the biochemical functions of BRCA1 are largely unknown.

The predominant BRCA1 mRNA of 8.0 kb encodes a 1863 amino acid protein with only a few sequence motifs suggestive of function (Miki et al., 1994). There are two highly conserved regions. The first is the 100 amino acid N-terminus which encodes a RING finger motif, a domain that is predicted to bind zinc and may be a protein–protein interaction motif (Borden et al., 1995; Lovering et al., 1993). The second region is at the C-terminus which contains an acidic region and two copies of a novel motif, designated the BRCT domain. The BRCT domain is present in a variety of putative cell-cycle related proteins, including RAD9 and 53BP1 (Koonin et al., 1996). The most abundant BRCA1 protein is apparently a ~220 kDa phosphoprotein which is predominantly, but apparently not exclusively, nuclear in subcellular distribution (Chen et al., 1995, 1996b; Scully et al., 1996). BRCA1 is localized to discrete nuclear dot structures in a cell-cycle-dependent manner (Scully et al., 1997b). Other isoforms of BRCA1 have been detected including a protein of 97 kDa. This smaller form lacks exon 11, and thus a functional nuclear localization signal, and is presumably the result of an alternative splicing event (Thakur

1098

et al., 1997). The above observations, coupled with the finding of a BRCA1 COOH-terminal domain capable of activating transcription as a Gal4 DNA-binding domain fusion (Chapman and Verma, 1996) and the co-fractionation of BRCA1 with the RNA pol II holoenzyme (Scully *et al.*, 1997a), suggest a role for BRCA1 in transcriptional regulation.

The expression patterns of *BRCA1* further support its role in growth regulation and/or differentiation. The spatial-temporal expression pattern in the embryonic mouse includes the neuroepithelium, and epithelial lineages of the skin, kidney and mammary gland (Marquis *et al.*, 1995). Moreover, *BRCA1* mRNA is sharply increased in alveolar and ductal cells of the breast epithelia during pregnancy (Marquis *et al.*, 1995). Consistent with this, *BRCA1* transcription is under (indirect) hormonal control in both cell culture and organismal systems (Gudas *et al.*, 1995, 1996; Vaughn *et al.*, 1996; Marks *et al.*, 1997). *BRCA1* is also highly expressed in the adult testis during the final stages of meiosis and spermiogenesis (Zabludoff *et al.*, 1996). Together, these observations suggest a broad role for BRCA1 in terminal differentiation events in multiple tissues. Somewhat paradoxically, the murine *brca1*−/− embryos die very early in gestation and exhibit severe cell proliferation defects and profound cell cycle arrest (Hakem *et al.*, 1996; Liu *et al.*, 1996). The association of *BRCA1* expression with both proliferation and differentiation events suggests a possible role for BRCA1 in regulating a genetic program which prepares the cell for terminal differentiation and possibly maintains that phenotype. Results of cell culture and transfection studies have underscored the tumor suppression function of BRCA1, but have revealed little of possible mechanisms. *BRCA1* antisense expression can transform fibroblasts and accelerates growth of breast cancer cell lines (Rao *et al.*, 1996; Thompson *et al.*, 1995). Expression of wild-type *BRCA1* inhibits colony formation and tumor growth *in vivo*, whereas tumor derived mutants of *BRCA1* lack this growth suppression activity (Holt *et al.*, 1996).

Evidence of a role for BRCA1 as a terminal differentiation checkpoint has recently been provided by the finding that BRCA1 and the RAD51 protein (involved in DNA recombination/repair) are co-localized and physically associated in mitotic and meiotic cells (Scully *et al.*, 1997b). The co-localization of BRCA1 and RAD51 on synaptonemal meiotic chromosomes suggests a role for this complex in either the fidelity of DNA replication, cell-cycle progression or genomic integrity. Though intriguing, these results do not suggest a function for BRCA1 which, when lost through mutation of the BRCA1 gene, would give rise to tumors. Strategies based upon identification of proteins which bind to BRCA1 have yielded components of the nuclear import pathway (Chen *et al.*, 1996a) and a novel RING finger/BRCT-domain-containing protein, BARD1 (Jin *et al.*, 1997; Wu *et al.*, 1996). However, none of these associated proteins have suggested a function for BRCA1.

We have chosen to focus upon the highly conserved BRCA1 RING finger domain as a potential protein–protein interface. This motif is defined by a spatially conserved set of cysteine–histidine residues of the form C_3HC_4. Structural analysis of the motif shows that two molecules of zinc are chelated by the consensus residues in a unique 'cross-braced' fashion (for reviews, see; Klug and Schwabe, 1995; Saurin *et al.*, 1996). Comparative structure analyses suggest that the RING fingers have a common hydrophobic core structure but that the region encoded by amino acids spanning cysteines 24 and 64 (for BRCA1) forms a highly variable loop structure which may be the determinant of protein–protein interaction specificity. The RING motif occurs in over 80 proteins including the products of proto-oncogenes and putative transcription factors (Saurin *et al.*, 1996). Evidence that the RING finger domain functions as a protein–protein interface has come from the study of the proto-oncogene PML (Borden *et al.*, 1995) and the transcriptional co-repressor KAP-1 (Friedman *et al.*, 1996). Intriguingly, like BRCA1, both PML and KAP-1 are localized to discrete, non-overlapping, nuclear dot structures, and mutations in the RING finger of PML abolish its localization to these dot structures (Borden *et al.*, 1995).

We hypothesize that the BRCA1 RING finger is a binding site for protein(s) which either mediate BRCA1 tumor suppressor function or serve to regulate these functions. Genetic evidence supports this in that single amino-acid substitutions at metal chelating cysteines, C61G and C64G, occur in *BRCA1* kindreds; these mutations segregate with the disease susceptibility phenotype and are predicted to abolish RING finger structure. We have used the yeast two-hybrid system to isolate proteins which bind to the wild-type BRCA1 RING finger but not to the C61G or C64G mutated RING fingers or other closely related RING fingers. We have isolated mouse and human clones of a novel protein, *BRCA1 associated protein-1* (BAP), which fulfils these criteria. BAP1 is a novel, nuclear-localized enzyme which displays the signature motifs and activities of a ubiquitin carboxy-terminal hydrolase. Full-length BRCA1 binds to BAP1 *in vitro* and enhances the growth suppression properties of BRCA1 in colony formation assays. The human *BAP1* locus was mapped to chromosome 3p21.3, and homozygous deletions of *BAP1* were found in non-small cell lung cancers. Together, these data suggest that *BAP1* is a key player in the *BRCA1* growth suppression pathway, and may itself be a tumor suppressor gene. The identification of BAP1 as a ubiquitin hydrolase implicates the ubiquitin-proteasome pathway in either the regulation, or as a direct effector, of BRCA1 function. BAP1 is the first nuclear-localized ubiquitin carboxy-terminal hydrolase to be identified, and may play a broad role in ubiquitin-dependent regulatory processes within the nucleus, including the emerging roles of ubiquitin conjugation as a post-translational modification which alters protein function and/or subcellular targeting.

Results

A yeast two-hybrid screen for BRCA1 RING finger interacting proteins

We constructed a synthetic *BRCA1* gene encoding the amino-terminal 100 amino acids of human BRCA1 using long oligonucleotides and PCR-mediated over-

lap-extension gene synthesis techniques (Madden *et al.*, 1991). Codon usage was optimized for expression in *E. coli* and *S. cerevisiae*. The resulting gene was fused to

the LexA DNA binding domain (Figure 1b). The negative control/specificity controls included: (1) the Cys61Gly, Cys64Gly, Met18Thr and Arg71Gly muta-
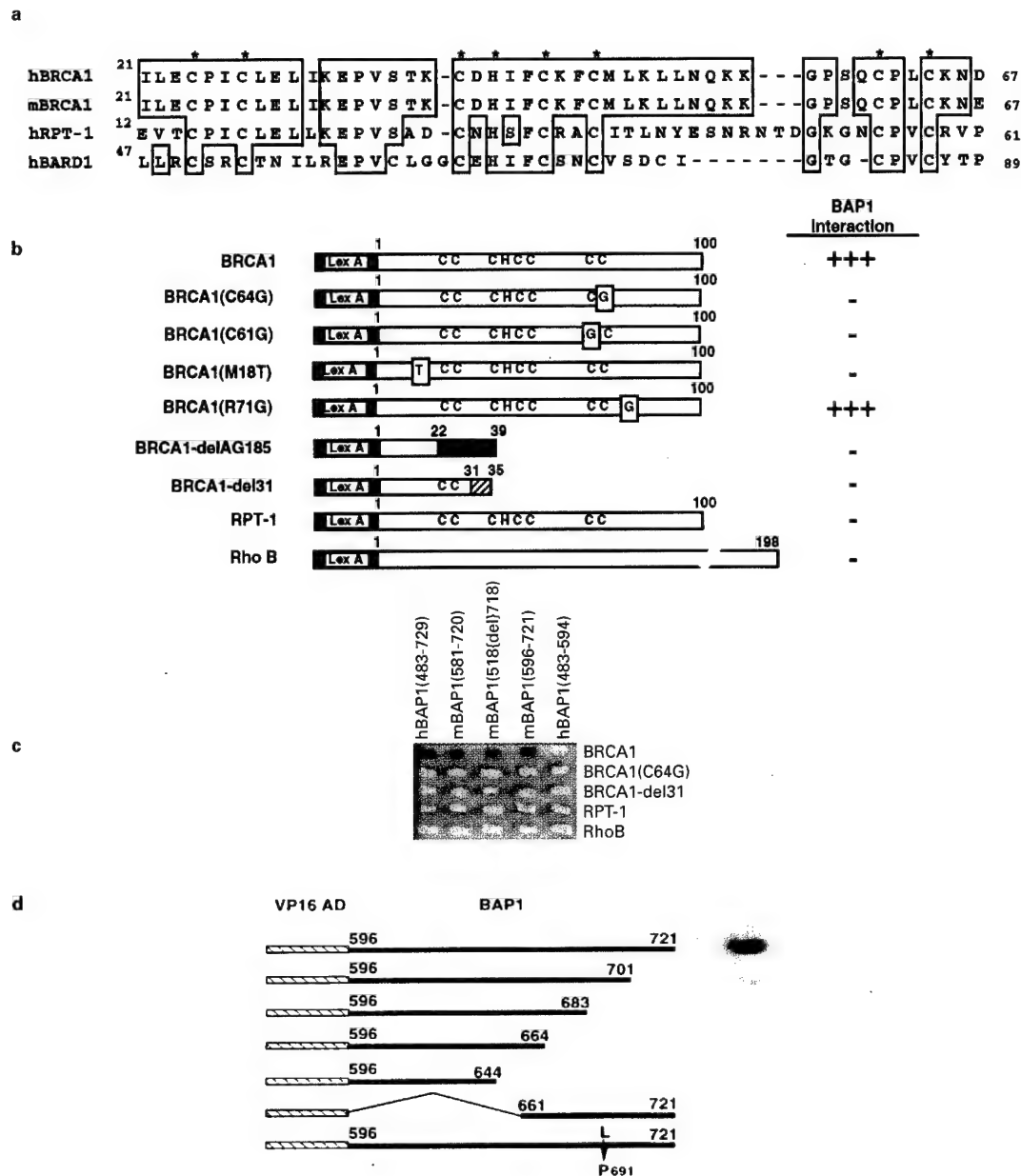

Figure 1 BRCA1 RING finger domain binds a novel protein. (**a**) Alignment of the RING finger domains of human and mouse BRCA1 (AA's 21–67), RPT-1 (AA's 12–61; the most closely related RING finger) and BARD1 (AA's 47–89). Asterisks (*) identify the Zn-chelating amino acids that form the core of the RING finger. Boxed amino acids show regions of identity between the RING finger domains of human BRCA1 and the other proteins. Alignment performed by CLUSTALW (Thompson *et al.*, 1994). (**b**) The amino-terminal 100 amino acids of human BRCA1 (which includes the RING finger domain) or the indicated amino acids of the various BRCA1–RF mutants and controls were fused to the LexA DNA-binding domain. Expression of all fusions in yeast was confirmed by Western analysis. A summary of the two-hybrid interaction between the Gal4-hBAP1(483–729) fusion clone and the various LexA-RING finger fusions is shown. (**c**) The BRCA1-interacting protein specifically interacts with the BRCA1 RING finger domain. Two hybrid screens of a human B-cell library and a mouse embryo (9.5–10.5 days) library identified a protein that interacted with wild type BRCA1–RF, but not with BRCA1-del31 (a truncated BRCA1), BRCA1(Cys64Gly) (a BRCA1–RF containing a point mutation), RPT-1 (a RING finger closely resembling the BRCA1), or RhoB (a non-related protein). Dark color of yeast indicates transcription from the LacZ reporter gene. Clones obtained from the two libraries are described as partial BAP1 proteins with AAs in parentheses. h, human; m, mouse. (**d**) The two-hybrid interaction between the BRCA1 RING domain and BAP1 requires the BAP1 C-terminal domain. Murine clone mBAP1(596–721) defines a portion of the BRCA1-interaction domain of BAP1. Mutants of this clone were generated by PCR-based deletion or point mutagenesis of mBAP1(596–721) as described in Materials and methods. Each individual mutant was co-transformed with LexA-BRCA1–RF into yeast and tested for interaction via its ability to activate transcription from the LacZ locus. Expression of all fusions in yeast were confirmed by Western analysis

tions that occur in *BRCA1* families; (2) the protein equivalent of the del AG185 mutation which results in a frame-shift at amino acid 22 followed by 17 out-of-frame amino acids and a stop codon; (3) a truncated BRCA1 RING finger at amino acid 31, the result of a PCR error; (4) the RPT-1 RING finger domain, a putative lymphocyte-specific transcription factor, whose RING finger domain is most highly related to
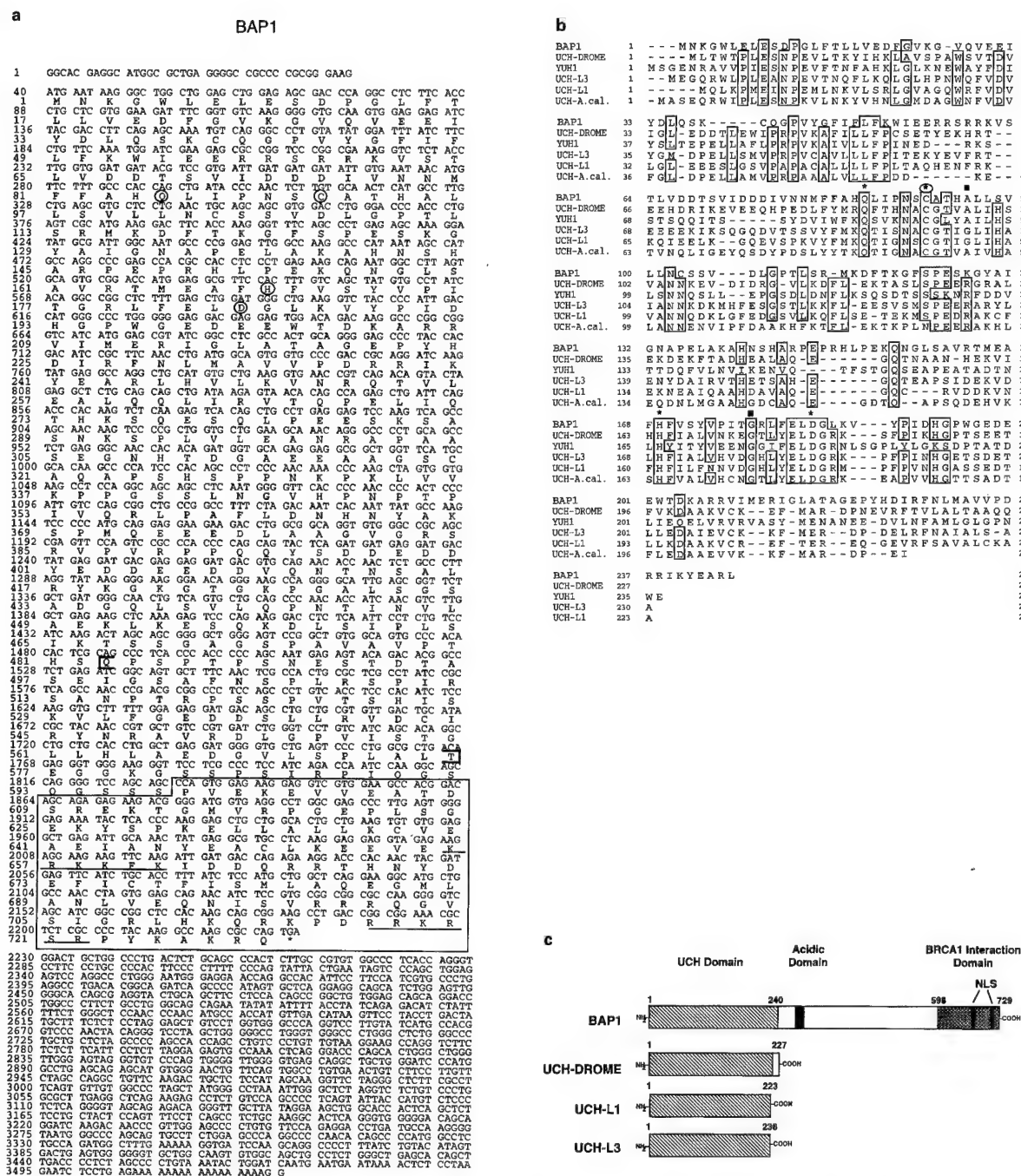
a

BAP1

b

c

Figure 2 BAP1 is a novel ubiquitin carboxy-terminal hydrolase (UCH). (**a**) The nucleotide and amino acid sequence of BAP1. The longest open reading frame which contained the amino acids defined by the human 2-hybrid fusion protein is 2188 nucleotides encoding 729 amino acids. The cDNA also contains 39 nucleotides of 5'UTR and 1295 nucleotides of 3'UTR. The enzymatic active site is contained within the first 250 amino acids; the active site residues are circled. The putative nuclear localization signals (NLS) are underlined, the BRCA1-interaction domain is boxed and the protein fragment used to generate BAP1 polyclonal antibodies is bracketed (AAs 483–576). (**b**) Comparison of BAP1 with other UCH's. UCH DROME (genebank #P35122), YUH1 (genebank #P35127), UCHL-1 (genebank #PO9936), UCHL-3 (genebank #P15374), UCH A.cal. (genebank #U90177). The BLAST search algorithm was used to identify proteins closely related to BAP1 (Altschul *et al.*, 1990). The UCH domain of five of these proteins were aligned with BAP1 using the CLUSTALW (ver.1.6) algorithm (Thompson *et al.*, 1994). Residues conserved between species with an identity of 85% or greater are boxed. Active site residues are denoted with asterisks. The catalytic cysteine is marked with a circled asterisk. (**c**) Diagrammatic comparison between BAP1 and some of the other UCH family members

that of BRCA1 (Patarca *et al.*, 1988); and (5) a LexA fusion with RhoB. The wild-type BRCA1 RING finger (BRCA1–RF) did not display intrinsic transcriptional activation function in yeast, and expression of each LexA fusion in yeast was confirmed by Western blot analysis with anti-LexA antibody (data not shown).

Guided by the expression patterns of BRCA1 during mouse development and in human spleen, we chose to screen cDNA libraries constructed from E9.5-10.5d whole mouse embryos and human adult B cells with the LexA-BRCA1–RF. Thirty-one cDNAs which specifically interacted with BRCA–RF were obtained: eight of these (three from the human library and five from the mouse library) encoded the same amino acid sequence. These were designated *BRCA1 Associated Protein-1* (BAP1) and pursued further. Each clone shares the same translational reading frame with respect to the transcriptional activation domain to which it is fused. In addition, the fusion junctions were different among the clones, suggesting that the interaction was not due to a fusion-junction artifact. Furthermore, the hBAP1 (483–729) and the BRCA1–RF interacted strongly in a mammalian two-hybrid assay (data not shown). The longest *BAP1* cDNA retrieved in the two-hybrid screen was a ~2.0 kbp clone from the human library and encoded 246 amino acids followed by a 1.3 kb 3′UTR. Each murine clone encoded an overlapping, smaller subset of this human open reading frame with a human-murine AA sequence identity of 100% over the COOH-terminal 100 AAs (data not shown). Both human and mouse clones showed a strong interaction with the wild-type BRCA1–RF and BRCA1 (Arg71Gly) substitution, but failed to interact with the C64G, C61G, del31, delAG, RPT-1, RhoB, or a variety of other LexA fusion constructs (Figure 1b,c and data not shown).

Further definition of this highly conserved interaction domain was performed by mutagenesis of this region of BAP1. Deletion of protein sequence from the carboxyl or amino termini of mBAP1(596–721) almost completely destroyed the BAP1-BRCA1 interaction (Figure 1d), possibly suggesting an extended interface between the proteins. Interestingly, the mBAP1(518del718) clone interacted most poorly with BRCA1–RF (Figure 1c) and lacked a 93 bp sequence (the reading frame was maintained), possibly the result of a naturally occurring splice variant. That BAP1 also failed to bind multiple, independent tumor-derived mutations of the BRCA1–RF provides strong evidence for the relevance of this interaction to the functions of BRCA1.

Analysis of the BAP1 cDNA

A full-length cDNA was constructed using two IMAGE consortium EST clones and RT–PCR (Figure 2a; see Materials and methods). The *BAP1* cDNA comprises 3525 bp; a polyA tract is present along with multiple polyA signals. Conceptual translation yields a long open reading frame of 729 amino acids with a predicted MW of 81 kDa and pI of 6.3. The presumptive initiator methionine is within a favorable context for translation start, however the short 5′UTR of 39 bp encodes amino acids in-frame with the presumptive methionine and does not contain
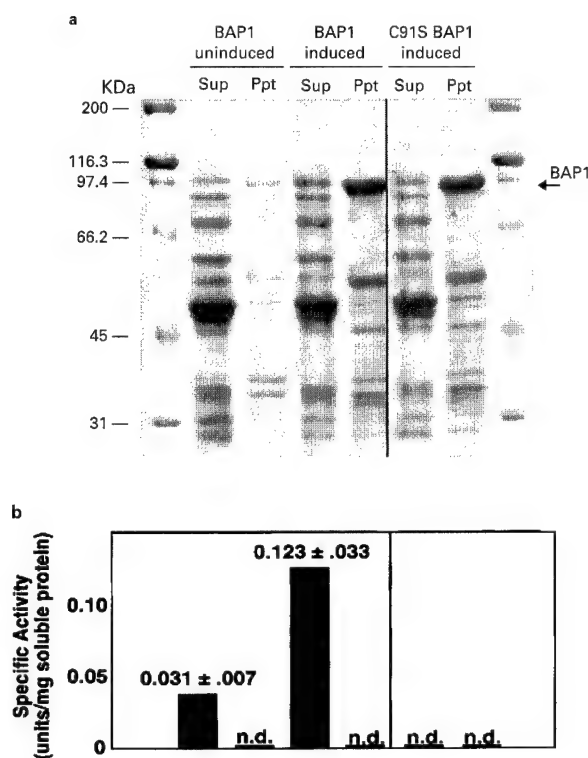

Figure 3 BAP1 has ubiquitin hydrolase activity. BAP1, or an enzymatically null mutant, BAP1(C91S), were expressed in bacteria by IPTG induction. Bacteria were harvested, lysed and supernatant (Sup) and pellet (Ppt) fractions generated. Each fraction was then measured for UCH activity (bar diagram; n.d., not detected). Induction of protein was verified by SDS–PAGE of each fraction. Arrow indicates BAP1 and BAP1(C91S) protein

a stop codon. Computer database searches indicated that BAP1 is a novel protein with the amino-terminal 240 amino acids showing significant homology to a class of thiol proteases, designated ubiquitin C-terminal hydrolases (UCH), which are implicated in the proteolytic processing of ubiquitin (Wilkinson *et al.*, 1989). These enzymes play a key role in protein degradation via the ubiquitin-dependent proteasome pathway. Similarities to other mammalian UCHs (UCH-L3 and UCH-L1) have been found (Figure 2b and c). Most importantly, the residues which form the catalytic site (Q85, C91, H169 and D184) are completely conserved, including the FELDG motif (Larsen *et al.*, 1996). In addition, a loop of highly variable sequence, which is disordered in the crystallographic structure of human UCH-L3 (Johnston *et al.*, 1997), is present (residues 140–167). This loop may occlude the active site or provide substrates specificity for the enzyme.

BAP1 has a number of additional motifs; a region of extreme acidity spanning amino acids 396 to 408, as well as multiple potential phosphorylation sites and N-linked glycosylation sites (Figure 2a). The C-terminal one-third is highly charged and is rich in proline, serine and threonine. The extreme C-terminus contains two putative nuclear localization signals, KRKKFK and RRKRSR and is hydrophilic, it is predicted to fold into a helical (possibly coiled-coil) structure (Figure 2a;
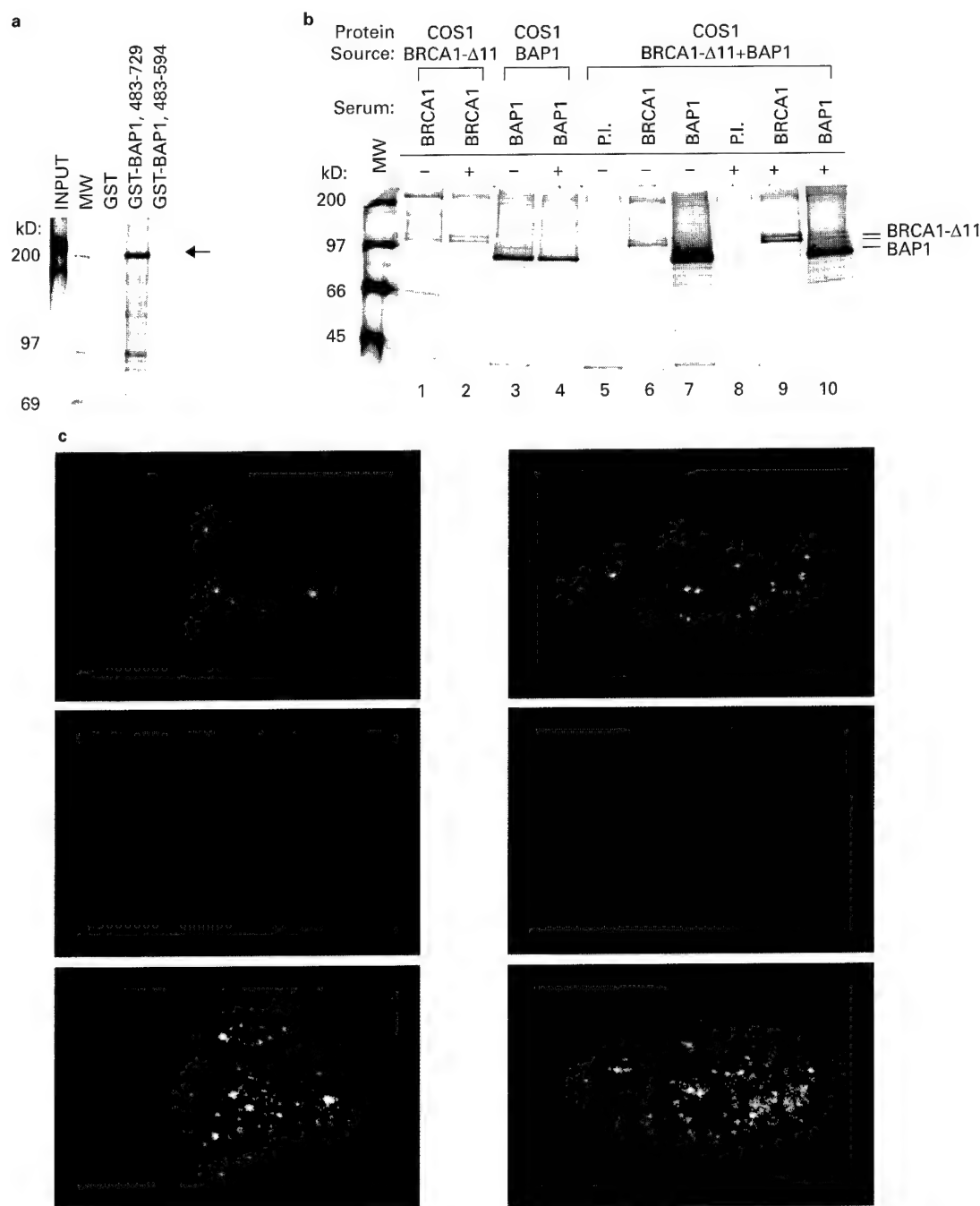
Figure 4 BAP1 and BRCA1 interact *in vitro* and *in vivo*. (a) BRCA1 and GST-hBAP1(483–729) interact *in vitro*. GST, GST-hBAP1(483–729) and GST-hBAP1(483–594) fusion proteins were expressed in *E. coli* and purified as described in Materials and methods. The Glutathione-Sepharose resins, containing an equivalent amount of fusion protein, were incubated in batch with *in vitro*-expressed, ^{35}S-labeled, BRCA1. After extensive washing, the proteins which remained bound were analysed by SDS–PAGE and fluorography. Lane 1, Input 2% of the labeled BRCA1 used in the associations with the glutathione resins. Lane 2, molecular weight markers. Lane 3, proteins bound to GST alone. Lane 4, proteins bound to GST-hBAP-1(483–729). Lane 5, proteins bound to GST-hBAP1-(483–594), a fusion protein lacking the BRCA1-interaction domain. Arrow indicates the BRCA1 protein. (b) Co-immunoprecipitation of BRCA1-Δ11 and BAP1. COS1 cells, transiently transfected with BRCA1-Δ11, BAP1, or BRCA1-Δ11 and BAP1 together, were treated with DMSO (−) or with 25 μM ALLN (+) for 16 h. Whole cell extracts were prepared after metabolic labeling and then immunoprecipitated with anti-BAP1 antibody (BAP1) or with anti-BRCA1 antibody, C20 (BRCA1) as indicated. Immunoprecipitated proteins were visualized by SDS–PAGE and fluorography. The BAP1 and BRCA1-Δ11 proteins are indicated. (c) BRCA1 and BAP1 partially co-localize in the nucleus. Asynchronous Rh30 cells were co-stained with the BRCA1-specific BR64 monoclonal antibody (green, top and bottom panels; Upstate Biotechnology) and a BAP1 specific, affinity-purified polyclonal antibody (red, middle and bottom panels). Top and middle panels are single color readouts of the dual color bottom panel. Yellow is produced where green and red images overlap

S Subbiah, personal communication). Indeed, within this domain the mutation of leucine 691 to a proline, a change predicted to disrupt the helical nature of this region, abolished the BAP1–BRCA1 interaction (Figure 1d). This result is consistent with the hypothesis that BAP1 uses a coiled-coil domain to interact with the RING finger domain of BRCA1. This overall architecture suggests that BAP1 is a new, structurally complex, nuclear-localized member of the UCH enzyme family.

BAP1 has UCH activity

To determine whether BAP1 did indeed have UCH enzymatic activity, BAP1 was expressed in bacteria and this protein was assayed for the ability to hydrolyze the glycine 76 ethyl ester of ubiquitin (Ub-OEt; Mayer and Wilkinson, 1989). IPTG-induced expression of BAP1 in bacteria led to abundant protein, most of which was found in an inactive, insoluble form (Figure 3a, 'BAP1 induced-Ppt'). The BAP1 protein found in the soluble

Figure 5 Tissue, spatial and temporal pattern of BAP1 expression. (a) Northern hybridization analysis of human RNA from multiple tissues. Northern blots that contain human RNA from the indicated tissues were probed with ^{32}P-labeled hBAP-1(483–729) cDNA (nts. 1488–3525). The blots were subsequently probed with a muscle actin cDNA. (b) Northern hybridization analysis of *Bap1* expression during mammary gland development. A Northern blot containing poly(A)$^+$ RNA isolated from mouse mammary glands at the indicated developmental stages was probed with ^{32}P-labeled mBAP1(596–721) cDNA. Note that mouse *Bap1* RNA is slightly smaller than the human *BAP1* RNA. (c) *In situ* hybridization analysis of *Bap1* expression. Bright-field (1, 3, 5, 7, 9 and 11) and dark-field (2, 4, 6, 8, 10 and 12) photomicrographs of *in situ* hybridization analyses performed on paraffin sections of mammary glands harvested from adolescent (1–4), mature (5, 6) or pregnant (9, 10) mice. Also shown are sections of testis (7, 8) and ovary (11, 12). To facilitate comparison, dark-field photomicrographs of breast were taken using identical shutter exposure times. al, alveolar bud; d, ductal epithelium; lu, ductal lumen; st, stroma; teb, terminal end bud; d, bm, basement membrane; se, semeniferous tubule; f, developing follicle; g, granulosa cells; th, thecal cells; ct, connective tissue

1104

fraction was able to hydrolyze Ub-OEt, indicating that BAP1 contains UCH-like enzymatic activity (Figure 3b). The active site thiol residue responsible for UCH activity in UCH-L3 has been identified and its mutation leads to abolition of enzyme activity (Larsen *et al.*, 1996). Mutation of the corresponding cysteine residue in BAP1, BAP1(C91S), yielded a protein with no detectable UCH activity (Figure 3b) further supporting the conclusion that BAP1 is a thiol protease of the UCH family.

BAP1 associates with BRCA1 in vitro *and* in vivo

Association of BRCA1 with BAP1 was tested *in vitro* by binding of full-length BRCA1 to hBAP1(483–729) fused to glutathione S-transferase (GST; Figure 4a). The ³⁵S-labeled BRCA1, produced by coupled *in vitro* transcription and translation, specifically bound to the GST–hBAP1(483–729) fusion protein, but not to GST alone (Figure 4a) indicating a physical association between the two proteins. As predicted from the yeast two-hybrid results (Figures 1d and 4a), BRCA1 did not bind to GST–hBAP1(483–594), a GST–BAP1 fusion protein lacking the BRCA1 interaction domain.

To determine whether BRCA1 and BAP1 could interact in mammalian cells, a co-immunoprecipitation analysis from co-transfected COS1 cells was performed (Figure 4b). Several attempts to transiently express BRCA1 to any significant level in COS1 cells were without success. Therefore, we performed the analysis with BRCA1-Δ11, a naturally occurring splice variant (Thakur *et al.*, 1997) which can be expressed in these cells and which contains the RING finger domain. The proteasome/caspase inhibitor ALLN (N-acetyl-L-Leucinyl-L-Leucinyl-L-norLeucinal) was included in the analysis to determine its influence on the stability of the interaction between BRCA1 and BAP1. BRCA1-Δ11 was detected by immunoprecipitation as a sharp band at ∼99 kDa in singly transfected COS1 cells (Figure 4b, lane 1). Incubation of a parallel set of transfected cells with ALLN (20 h) prior to harvest revealed a discrete slower migrating band in the anti-BRCA1 immunoprecipitates (Figure 4b, lane 2). Immunoprecipitates from BAP1-transfected COS1 cells revealed a 91 kDa protein whose mobility was apparently unaffected by treatment with ALLN (Figure 4b, lanes 3 and 4). Co-transfection of COS1 cells with BRCA1-Δ11 and BAP1 revealed that these proteins could be co-immunoprecipitated using either anti-BAP1 or anti-BRCA1 antibodies (Figure 4b, lanes 9 and 10); the ability to detect the BRCA1–BAP1 complex under these conditions was dependent upon incubation of the cells with the proteasome inhibitor. In co-transfected, ALLN-treated cells, both forms of BRCA1-Δ11 are evident in the co-immunoprecipitated complex, and both forms are more abundant than singly transfected cells (compare lanes 2 and 10). These results demonstrate the *in vivo* association of BRCA1 and BAP1, and suggest the presence of a proteasome inhibitor-sensitive modification of BRCA1 which may enhance its interaction with BAP1.

To further document the *in vivo* interaction between BAP1 and full-length BRCA1, we determined whether the endogenous (non-transfected) proteins were co-localized in the cell nucleus (Figure 4c). A mouse monoclonal antibody to BRCA1 (Maul *et al.*, manuscript in preparation) and affinity purified rabbit BAP1 antibody were used to stain rhabdomyosarcoma cells (Rh30), a cell line previously determined to express *BAP1* RNA (Jensen and Rauscher, unpublished results). BRCA1 was detected exclusively in punctate domains within the nucleus (excluding nucleoli) in agreement with other reports (Jin *et al.*, 1997; Scully *et al.*, 1997b). BAP1 was also detected in punctate domains within the nucleus of Rh30 cells, however, the number of domains was significantly greater than for BRCA1. Several of the BRCA1 domains coincided with BAP1 domains (yellow dots in the bottom panels), suggesting an endogenous BRCA1-BAP1 interaction. We also detected BRCA1 reactive domains which were not co-localized with BAP1 domains as has been seen with other BRCA1-interacting proteins (Figure 4c; Jin *et al.*, 1997; Scully *et al.*, 1997b). These data show that BAP1 and BRCA1 can physically interact *in vitro* and *in vivo*, and have overlapping subnuclear expression patterns.
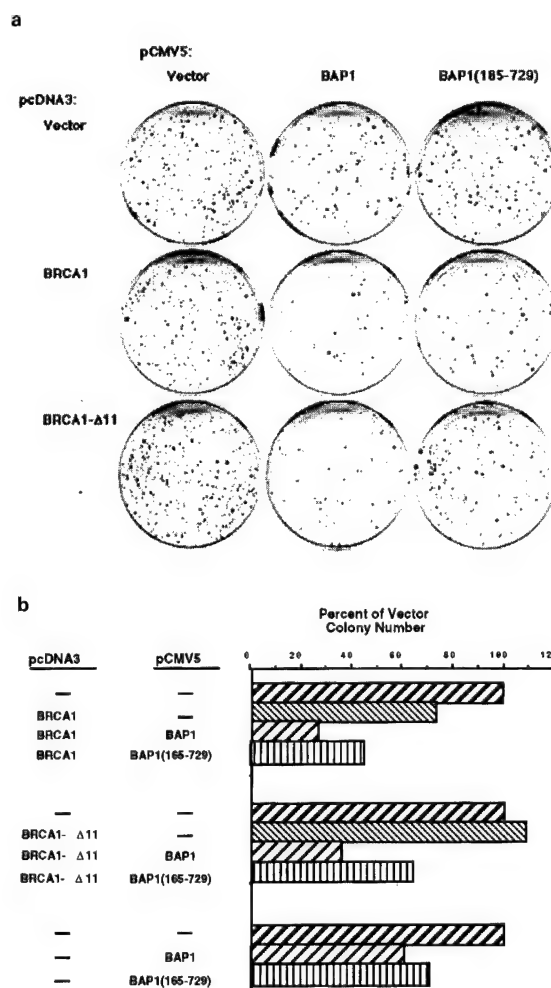
a

b

Figure 6 BAP1 enhances BRCA1-mediated growth suppression. (a) MCF7 cells were co-transfected with each of the plasmid constructs shown. Cells were then harvested and 5×10^5 cells were plated in duplicate into complete medium containing G418. Twenty-one to 28 days later, cells were stained and colonies counted. The experiment was repeated four times with similar results. (b) Quantitation of the results from (a)

BAP1 is expressed in a temporal and spatial pattern during breast development/remodeling

The physical interaction between BAP1 and BRCA1 suggests that the proteins might be expressed in similar tissues. Northern blot hybridization analysis of *BAP1* expression in a variety of human adult tissues indicated that human *BAP1* was encoded by a single mRNA species of ∼4 kb in all tissues except testis, where a second, ∼4.8 kb mRNA, was also detected (Figure 5a). High expression was detected in testis, placenta and ovary, with varying levels detected in the remaining tissues. Expression of *BAP1* in normal human breast tissue was detected by RT–PCR of total RNA isolated from normal human mammary epithelial cells (data not shown).

Northern analysis and *in situ* hybridization were performed to determine whether the spatial and temporal pattern of *Bap1* expression in the breast corresponded to that previously described for *Brca1* (Figure 5b and c; Marquis *et al.*, 1995). *Bap1* was expressed at slightly higher levels in the mammary glands of 5 week-old adolescent female mice compared to 15 week-old mature mice. Consistent with this, *in situ* hybridization revealed high level of *Bap1* mRNA expression in terminal end buds (Figure 5c), and higher levels of *Bap1* expression in the ductal epithelium of adolescent as compared with mature female mice. Like *Brca1*, *Bap1* mRNA was expressed in the mammary epithelium at levels higher than those found in the stromal compartment. Steady-state levels of *Bap1* mRNA were up-regulated in the mammary glands of pregnant mice (Figure 5b and c). Like *Brca1*, *in situ* hybridization demonstrated that this up-regulation occurred predominantly in developing alveoli (Figure 5c). *Bap1* was expressed at higher levels in the mammary glands of parous animals that had undergone 28 days of post-lactational regression as compared with age-matched virgin controls (cf. D28 regression and 15 week virgin). The observation that *Bap1* expression is up-regulated in the breast during puberty, pregnancy and as a result of parity is similar to that previously made for *Brca1* and suggests the developmental co-expression of these two proteins (Marquis *et al.*, 1995). It should be noted, however, that the magnitude of *Bap1* up-regulation at each of these developmental stages was lower than that observed for *Brca1*. The spatial distribution of *Bap1* expression was also investigated in the testis and ovary (Figure 5c). Like *Brca1*, *Bap1* was expressed at high levels in semeniferous tubules, with lower levels of expression observed in the surrounding connective tissue. *Bap1* was also expressed at high levels throughout the ovary.

BAP1 augments the growth suppressive activity of BRCA1

Several studies have shown that BRCA1 can affect the growth characteristics of cells (Holt *et al.*, 1996; Rao *et al.*, 1996). We determined whether BAP1 itself may affect cell growth or may alter BRCA1-mediated changes in cell growth. *BRCA1* and *BAP1* cDNAs were co-transfected into MCF7 breast cancer cells and analysed for their effect on colony formation (Figure 6). This cell line was chosen for several reasons: First,
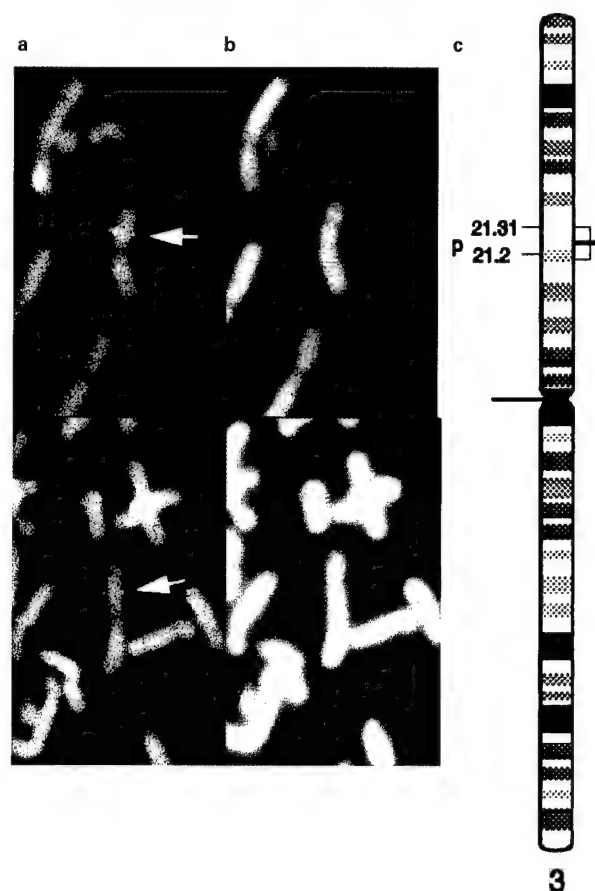

Figure 7 *BAP1* maps to Chromosome 3p21.3. Fluorescence *in situ* hybridization (FISH) of partial metaphases using biotin-labeled BAP1 cDNA. (**a**) the specific FISH signals on chromosome 3 (arrows), with (**b**) the simultaneously DAPI-stained chromosomes and (**c**) a chromosome ideogram with the localization of BAP1 based on the DAPI-band pattern and FLpter value. The horizontal box indicates the variation in FLpter values on individual chromosomes

it previously has been shown that the growth of these cells is inhibited by the overexpression of *BRCA1* (Holt *et al.*, 1996). Second, both Northern and RT–PCR analyses showed that BAP1 is expressed in this cell line (data not shown). Finally, RT–PCR/SSCP analysis of the open reading frame of *BAP1* cDNA prepared from this cell line showed no mutations (data not shown).

The expression of BRCA1 alone (BRCA:pCMV5) decreased the number of colonies formed by these cells when compared to the vector control (pcDNA3:pCMV5), in agreement with other studies (Holt *et al.*, 1996). The co-expression of BRCA1 and BAP1 (BRCA1:BAP1) significantly decreased the number of cell colonies (approximately fourfold *vs* BRCA1 alone; see Figure 6b) indicating that BAP1 enhances the growth suppressive actions of BRCA1. A mutant of BAP1, BAP1(165–729), in which the enzymatic region is deleted but which still binds to BRCA1, also enhanced the growth suppression of BRCA1, but not to the same extent as the wild-type BAP1.

The expression of BRCA1-Δ11 (a naturally occurring splice variant of BRCA1) in MCF7 cells by itself had no effect on the growth of MCF7 cells (Figure 6).

However, the co-expression of BRCA1-Δ11 and BAP1 dramatically decreased the number of colonies, suggesting that the presence of BAP1 could cooperate with BRCA1-Δ11 in cell growth inhibition. Furthermore, the expression of BAP1 in MCF7 cells also reduced the number of colonies formed (pcDNA3:BAP1; see Figure 6b). The expression of the enzymatic mutant, BAP1(165–729), alone or in combination with BRCA1-Δ11, yielded no growth-suppression activity. Thus, enzymatically active BAP1 enhances BRCA1-mediated suppression of growth in this assay.

BAP1 is located on chromosome 3p21.3 and is mutated in non-small cell lung carcinoma

The data above suggest the possibility that *BAP1* itself may be a tumor suppressor gene and that *BAP1* alterations/deletions might play a role in human tumorigenesis. We determined whether *BAP1* might be located at a chromosomal region previously observed to be mutated in human cancers. The full-

length *BAP1* cDNA was used in fluorescent *in situ* hybridization (FISH) to identify the chromosomal location of the *BAP1* gene (Figure 7). Specific signals were observed only on the midportion of the short arm of chromosome 3 with 42 of 69 analysed metaphase spreads showing at least one specific signal. The FLpter value was 0.27 ± 0.02 corresponding to a localization for *BAP1* at 3p21.2-p21.31. This location is a region of LOH for breast cancer as well as a region frequently deleted in lung carcinomas (Buchhagen *et al.*, 1994; Thiberville *et al.*, 1995).

The chromosomal location of *BAP1* suggested the possibility of mutations within *BAP1* in lung tumors. Thus, a total of 44 small cell lung cancer (SCLC), 33 non-small cell lung cancer (NSCLC) and two lymphoblastoid tumor cell lines were screened for mutations within the *BAP1* gene by Southern, Northern and PCR-based SSCP analyses. Genomic DNAs from 15 small cell lung cancer (SCLC), 18 non-small cell lung cancer (NSCLC) and two lymphoblastoid cell lines (representing a subset of the total), were subjected to *Eco*RI digestion and then hybridized to a full-length
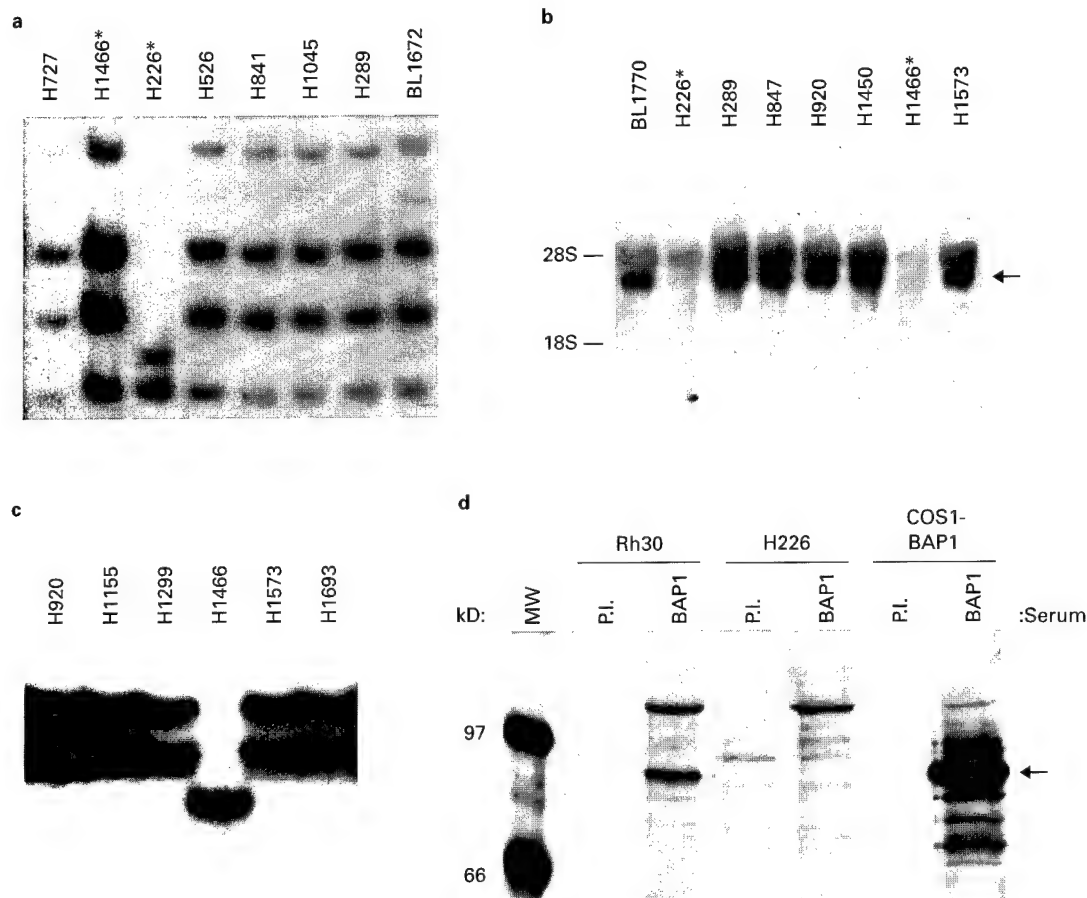

Figure 8 Mutational analysis of lung carcinomas. (**a**) Southern blot hybridization with *Bam*HI digestion showing four distinct bands at 7.5 kbp, 4.0 kbp, 3.0 kbp and 2.4 kbp as detected by a full-length BAP1 probe. The non-small cell lung cancer NCI-H226 line shows an absence of the 7.5 kbp, 4.0 kbp and 3.0 kbp bands. An aberrant 2.6 kbp band is detected in the NCI-H226 cell line. (**b**) Northern blot hybridization showing a ~4 kb message (arrow) which is absent in the NCI-H226 cell line and the non-small cell lung cancer NCI-H1466 cell line. A fainter (5.0 kb) band is visible corresponding to cross hybridization with the 28S ribosomal component. (**c**) SSCP analysis showing a homozygous shift in H1466 detected by RT–PCR amplification spanning nts 1089 to 1286. (**d**) BAP1 is a 90 kD protein and is missing from NCI-H226 cells. Endogenous BAP1 from Rh30 or H226 cells, or BAP1 expressed in COS1 cells from the BAP1 cDNA, was immunoprecipitated from whole cell lysates prepared after ^{35}S-labeling of 1×10^7 cells. Immunoprecipitated proteins were analysed by SDS–PAGE followed by fluorography. The arrow indicates the BAP1 protein. All cell lines in panels **a**, **b** and **c** are listed by their NCI number (Phelps *et al.*, 1996)

BAP1 cDNA probe. A single 23 kb band was detected in the lymphoblastoid and most tumor cell lines (data not shown). One NSCLC line, NCI-H226, did not show the 23 kbp band but did show an aberrant 30 kbp band (data not shown). This abnormality was confirmed by *Bam*HI, *Xba*I, *Pst*I and *Bgl*II digestions. Using the 3.5 kbp BAP1 cDNA probe with *Bam*HI digested genomic DNAs, we detected four distinct bands at 7.5 kbp, 4.0 kbp, 3.0 kbp and 2.4 kbp which were present in all cell lines tested with the exception of NCI–H226 (a representative subset is shown in Figure 8a). In the NCI-H226 line, we detected only the 2.4 kbp band and an aberrant 2.6 kbp band.

Further mutational analysis of BAP1 was performed by screening a subset of 31 SCLC and 27 NSCLC lung cancer cell lines and two lymphoblastoid cell lines for expression of *BAP1* mRNA. Northern analysis showed that most cell lines expressed a single ~4 kb mRNA (Figure 8b). However, two cell lines, NCI–H226 and NCI–H1466 (both NSCLCs), showed undetectable levels of *BAP1* expression, suggesting that *BAP1* may be a target for inactivation or down-regulation during NSCLC pathogenesis. The absence of BAP1 protein in the NCI–H226 line was determined by immunoprecipitation of BAP1 from ^{35}S-labeled cells (Figure 8d).

We screened cDNAs from all 44 SCLC and 33 NSCLC cell lines for mutations in the BAP1 open reading frame by RTPCR–SSCP (Figure 8c). A homozygous, eight base pair deletion and a presumed splice variant were detected. An 8 bp deletion was detected in the cDNA from the NSCLC line NCI–H1466; This short deletion leads to a frameshift/ truncation yielding a predicted 393 amino acid protein. This homozygous deletion was confirmed in genomic DNA from the same cell line (data not shown). A 54 bp in-frame deletion (nts. 705–758) was detected in the NCI–H1963 (SCLC) cell line. This deletion was heterozygous at the cDNA level and not present in the genomic DNA, suggesting that it is a splice variant. However, this variant was not detected in any of the other cell lines screened. These data clearly show that genetic alterations, including intragenic homozygous deletions, can occur in *BAP1*.

Discussion

We have discovered and characterized a novel protein, BAP1, which binds to the BRCA1 RING finger motif. Several lines of evidence are offered which support a role for BAP1 in BRCA1 signal transduction pathways. We showed that: (1) BAP1 binds to the RING finger of BRCA1; but not to germline mutants of BRCA1 or related RING domains; (2) The BAP1– BRCA1 interactions occurs *in vitro* and *in vivo*, and these proteins are partially co-localized in nuclear dot structures; (3) *BAP1* mRNA is expressed in those tissues which also expresses *BRCA1*, and the spatial/ temporal distribution of *Bap1* expression in the mouse breast is very similar to that observed with *Brca1*; (4) BAP1 enhances BRCA1-mediated suppression of cell growth in colony formation assays, and suppression by BAP1 is augmented by its UCH enzymatic domain; and (5) *BAP1* maps to chromosome 3p21.3 and is homozygously deleted in a lung carcinoma cell line. Together, these observations suggest that *BAP1* may

be a tumor suppressor gene, and that it may serve as a regulator of (or is an effector for) BRCA1 growth control/differentiation pathways. The specificity of the BRCA1 RING finger-BAP1 interaction and the fact that independent, germline missense mutations in the BRCA1 RING finger domain abolish interaction with BAP1 provide substantial evidence for the physiological relevance of this interaction.

BAP1 is a nuclear-localized, ubiquitin carboxy-terminal hydrolase (UCH) which can cleave model ubiquitin substrates *in vitro*. The UCH homology of BAP1 implies a role for either ubiquitin-mediated, proteasome-dependent degradation or other ubiquitin-mediated regulatory (Isaksson *et al.*, 1996) pathways in BRCA1 function. Regulated ubiquitination of proteins and subsequent proteasome-dependent proteolysis plays a role in almost every cellular growth, differentiation and homeostatic process (reviewed by Ciechanover, 1994; Isaksson *et al.*, 1996; Wilkinson, 1995). The pathway is regulated both at the level of substrate specificity – via the concerted actions of activating enzymes, carrier proteins and ligation enzymes – and at the level of proteolytic deuibiquitation and ubiquitin hydrolysis. The latter enzymes are ubiquitin-specific thiol proteases which have been broadly classified into two families: the ubiquitin-specific protease (UBPs) and the ubiquitin carboxy-terminal hydrolases (UCHs).

The UBP family members are 50–300 kDa, cytoplasmic or nuclear-localized proteins which, in general, cleave ubiquitin or ubiquitin-conjugates from large substrates. Such enzymatic activity can be found directly associated with the 26S proteasome and may serve a regulatory function by editing ubiquitin on large substrates or cleaving polyubiquitin, thus replenishing ubiquitin pools (Lam *et al.*, 1997). Remarkably, a number of UBPs have been isolated as growth regulatory and/or developmental control genes such as DOA4 in yeast, which controls DNA replication and repair (Papa and Hochstrasser, 1993); UBP3 which is involved in transcriptional silencing in yeast (Moazed and Johnson, 1996); the TRE2 oncogene which is mutated in the UBP active site and functions as a dominant negative transforming gene (Nakamura *et al.*, 1992); the drosophila *Fat Facets* gene which controls pattern formation and eye development (Huang *et al.*, 1995; Huang and Fischer-Vize, 1996); and the human DUB family of cytokine-inducible UBPs which control hematopoietic differentiation (Zhu *et al.*, 1996, 1997).

By contrast, the UCH family has been characterized as a set of small (25–30 kDa) cytoplasmic proteins which prefer to cleave ubiquitin from ubiquitin-conjugated small substrates and may also be involved in the co-translational processing of proubiquitin. Like the UBPs, UCHs show considerable tissue specificity and developmentally-timed regulation (Wilkinson *et al.*, 1992). UCH family members are differentially expressed in neuronal, hematopoietic and germ cells in many species. Most remarkably, a novel UCH enzyme has recently been cloned from *A. californica* whose enzymatic function is essential for acquisition and maintenance of long-term memory (Hedge *et al.*, 1997). Finally, UCH levels are down-regulated during viral transformation of fibroblasts (Honore *et al.*, 1991), consistent with a role in growth control.

BAP1 is the newest member of the UCH family and considerably expands the potential roles of this family of proteases. BAP1 is a much larger protein (90 kDa) and is the first nuclear-localized UCH. In addition to containing the ~ 250 amino acid amino-terminal UCH catalytic domain, it includes a carboxy-terminal extension rich in proline, serine and threonine, and a short, highly acidic region; these elements may confer a short half-life upon the protein (Rechsteiner and Rogers, 1996). The extreme carboxy-terminus encodes two potential nuclear localization signals that overlap the approximately 125 amino acid BRCA1-interaction domain. This domain is predicted to fold into a long amphiphatic helix of coiled-coil character, the structure of which may be important for BRCA1 interaction. Indeed, truncation into this region or substitution of a proline for leucine (L691P) abolish the BAP1–BRCA1 interaction in the two-hybrid assay. We have also detected a potential splice variant in BAP1 that results in loss of 31 amino acids of the BRCA1 interaction domain and greatly reduces the ability of BAP1 to bind the BRCA1 RING finger. Thus, our data suggest that the BAP1 carboxy-terminus is tethered to the BRCA1 RING finger domain, leaving the UCH catalytic domain free to interact with ubiquitinated, or other ubiquitin-like, substrates.

A simple model explaining most of our data is that BRCA1 is a direct substrate for the UCH activity of BAP1 and deubiquitination results in the stabilization of BRCA1. Thus, in contrast to the known UCHs which are comprised entirely of the UCH domain, the carboxy-terminal extension of BAP1 may provide substrate and/or targeting specificity for the catalytic function. Paradigms for separate substrate recognition and catalytic domains occur throughout the ubiquitin conjugation/ligation system (see Wilkinson, 1995 and references therein). Regulated ubiquitination of BRCA1 and subsequent proteasome-mediated degradation would be consistent with tight regulation of BRCA1 levels and its subnuclear localization during both the mitotic cell-cycle and meiosis (Gudas et al., 1996; Scully et al., 1997b; Zabludoff et al., 1996). Thus, BAP1-mediated deubiquitination of BRCA1 would stabilize the protein and protect it from proteasome-mediated degradation. This scenario is consistent with both the ability of co-transfected BAP1 to enhance the tumor suppressor effects of BRCA1 in colony formation assays and the finding of mutations in BAP1 in cancer cell lines.

A second, and equally plausible hypothesis is that the BRCA1–BAP1 association serves to target the UCH domain to other substrates that may be bound to other sites on BRCA1. In this scenario, BRCA1 may function as an assembly or scaffold molecule for regulated assembly of multiprotein complexes; a function that has been postulated for other tumor suppressor proteins (e.g. pRb; Sellers and Kaelin, 1996; Welch and Wang, 1995). Thus, BAP1 could be a regulator of this assembly via its control of ubiquitin-mediated proteolysis. Recently, it has been shown that the RING finger protein Ste5 (S. cerevisiae) functions as a scaffold protein for assembling protein kinase-dependent signaling complexes in pheromone signaling; this activity is abolished by mutations in the Ste5 RING finger (Inouye et al., 1997). In this context, two other RING finger-containing proteins are involved in

complexes whereby controlled proteolytic processes are dependent upon the integrity of the RING finger structure: (1) The murine homologue of the drosophila *seven-in-absentia*, siah, (a RING finger protein) binds to the tumor suppressor protein Deleted in Colon Cancer (DCC) and targets it for proteasome-mediated degradation. This degradation requires the siah RING finger structure (Hu et al., 1997); and (2) The herpesvirus protein VMW110 is a RING finger protein that binds directly to a UBP family member, HAUSP, and appears to target it to the ND10/POD nuclear dot structure. The ND10 structure itself contains another RING finger protein, the proto-oncogene PML (Everett et al., 1997). Remarkably, the PML RING finger has been shown to bind and co-localize with a ubiquitin-like molecule PIC1/SUMO1 which is emerging as a central molecule in nuclear-localized ubiquitin-dependent regulation (Saitoh et al., 1997).

A third hypothesis is that BAP1 is involved in the regulation of protein subcellular localization. Mono-ubiquitination, or addition of a ubiquitin-like moiety, has emerged as an important post-translational modification which may affect the specific targeting of proteins to locations other than the proteasome. For example, the addition of the ubiquitin-like PIC1/SUMO1 protein appears to mediate the movement of RanGAP1 (a GTPase-activating protein) from the cytoplasm to the nuclear envelope where it binds the RanBP2 protein (Mahajan et al., 1997). This interaction requires the ATP-dependent, covalent addition of PIC1/SUMO-1 to RanGAP1, a process extremely similar to the ATP-dependent, ubiquitin-ligation mechanism. Thus, BAP1-mediated removal of ubiquitin, or ubiquitin-like molecules, from BRCA1, or a protein associated with BRCA1, could target the complex to another cellular compartment, thus altering its function without physically destroying it. That BRCA1 is targeted to specific subcellular sites is evidenced by the observation that it accumulates in nuclear dot structures during S phase of the cell cycle. This localization is abolished at the S/G2 boundary (Scully et al., 1997b).

The association of BRCA1 with RAD51 in both mitotic nuclear dot structures and meiotic cells broadly implicates BRCA1 in DNA repair and/or recombination processes. The RAD51/52-dependent DNA repair pathway is highly regulated and includes many proteins, some of which may be potential substrates for BAP1-mediated ubiquitin hydrolysis. RAD23, which associates with the RAD51/52 complex, contains an amino-terminal ubiquitin-like domain which is required for RAD23 function and double-strand break repair (Watkins et al., 1993). Recently, a human ubiquitin-like protein, UBL-1, was isolated as a protein which binds directly to the human RAD51/RAD52 complex (Shen et al., 1996b). Interestingly, the yeast homologue of UBL1 is SMT3, which functionally associates with the yeast centromere protein MIF2, a protein required for proper chromosome segregation (Brown, 1995; Brown et al., 1993). Furthermore, the RAD51/52 complex contains a ubiquitin conjugating enzyme, hUBC9/UBE2I (Jiang and Koltin, 1996; Shen et al., 1996a). Thus, it appears that the DNA repair machinery contains both ubiquitin-conjugating and -hydrolyzing

elements, since BAP1 is now implicated as a member of the BRCA1/RAD51/hUBC9 complex. It is possible that BAP1, which is co-expressed with BRCA1 in breast tissue, may regulate the recombination/repair functions of the BRCA1/RAD52 complex by targeting either RAD23 or UBL1 for ubiquitin hydrolysis.

The implications that BAP1 is a key regulator and/or effector of BRCA1 suggest that BAP1 may also play a role in human cancer. The finding that *BAP1* maps to human chromosome 3p21.3 strongly suggested this link; Loss of chromosome 3p genes is a critical event in lung cancer pathogenesis and other carcinomas. Interestingly, two other components of the ubiquitin metabolism pathway have been mapped to chromosome 3p21.3; an ubiquitin activating enzyme (Kok *et al.*, 1993) and a ubiquitin protease, UNP (Gray *et al.*, 1995). The identification of BAP1 as a UCH suggests a cluster of metabolically related enzymes at this locus. Furthermore, the frequent loss of this chromosomal region suggests that there may be a selective advantage for the loss of ubiquitin-mediated cellular processes during carcinogenesis. That BAP1 may be included in this paradigm is suggested by our detection of rearrangements/deletions within BAP1 in lung cancers (this report) and our detection of independent, homozygous, point mutations in highly conserved residues of BAP1's enzymatic domain (Proctor *et al.*, manuscript in preparation).

In summary, we have isolated a novel ubiquitin hydrolase which associates directly with the BRCA1 RING finger domain. BAP1 may play a key role in ubiquitin-dependent regulatory processes in the nucleus including transcription, chromatin remodeling, cell cycle control and DNA repair/recombination.

Materials and methods

Cell culture, transfections and colony formation assays

All cells were grown at 37°C and 5% CO_2. COS1 and MCF7 cells were maintained in DMEM supplemented with 10% fetal bovine serum (FBS), L-glutamine and non-essential amino acids. Small cell lung cancer (SCLC) and non-small cell lung cancer (NSCLC) cell lines were maintained in RPMI media with 10% fetal bovine serum (Gibco BRL). Rh30 cells were maintained in RPMI supplemented with 10% FBS and non-essential amino acids. COS1 cells were transfected using DOSPOR transfection reagent (Boehringer Mannheim Biochemicals) following the manufacturer's protocol.

Colony formation assay

MCF7 cells were transfected by a modified $CaPO_4$-DNA precipitation method (Holt *et al.*, 1996). MCF7 cells, at 2×10^6 cells/10 cm dish, were fed fresh medium approximately 3 h prior to transfection, and were then treated with the Ca-DNA precipitate for 4 h. The cells were subjected to a brief shock with transfection buffer containing 15% glycerol. Twelve to 16 h later, the cells were trypsinized, counted and plated directly into complete medium containing 0.75 mg/mL G418 at 5×10^5 cells per 10 cm dish. Cells were fed fresh medium containing G418 every 3–4 days. Cells were stained for colonies approximately 21–28 days after transfection.

Yeast 2-hybrid

The yeast 2-hybrid system as modified by Stan Hollenberg was used for all yeast experiments (Vojtek *et al.*, 1993). Two libraries were screened for interaction with LexA-BRCA1; a human B cell, oligo-dT-primed, cDNA library (Durfee *et al.*, 1993); a kind gift from Dr Steve Elledge) and a mouse embryo (9.5–10.5 day), random-primed, cDNA library size selected for inserts of 300–500 base pairs in length (Vojtek *et al.*, 1993); a kind gift of Dr Stan Hollenberg).

Construction of expression plasmids

LexA fusion constructs: The 100 amino acid terminal region of human BRCA1 (BRCA1-RF) was used as the bait to screen for interacting proteins. All LexA fusion constructs were made by cloning the appropriate RING (or other) domain into the vector pBTM-116 (Vojtek *et al.*, 1993). A synthetic gene of the BRCA1–RF domain was made from overlapping oligonucleotides whose codon usage had been optimized for expression in *E. coli* and *S cerevisiae* (Madden *et al.*, 1991). Double-stranded DNA was generated by the Polymerase Chain Reaction (PCR) and amplified with flanking primers containing *Eco*RI and *Sal*I enzymatic restriction sites. A 'wild type' BRCA1–RF domain was confirmed by DNA sequencing. The single amino acid substitutions in the BRCA1–RF domain, BRCA1(C64G) (Cys 64 to Gly), BRCA1(C61G) (Cys 61 to Gly), BRCA1(M18T) (Met18Thr) and BRCA1(R71G) (Arg71 to Gly) as well as the BRCA1–delAG185 truncation mutant were created by PCR-mutagenesis (Ho *et al.*, 1989). The BRCA1-del31 truncation mutant was a mis-primed PCR reaction of the BRCA1–RF which was identified by DNA sequencing. The LexA-RPT-1 protein (amino acids 1–100) was made by PCR-mediated amplification of the corresponding nucleotides of a RPT-1 PCR sample (Patarca *et al.*, 1988); kindly provided by Dr Harvey Cantor). All clones were confirmed by sequencing. Expression of all constructs in yeast was confirmed by Western analysis using antibodies against the LexA DNA-binding domain (data not shown).

BAP1 constructs: A full-length BAP1 cDNA was assembled through the fusion of two overlapping EST clones (the IMAGE Consortium (LLNL); cDNA Clones #46154 and #40642; (Lennon *et al.*, 1996)) and the insertion of 62 nucleotides missing from clone #40642 (as revealed by sequencing and RT–PCR analyses). GST-hBAP1(483–729) was generated by cloning the *Xho*I fragment of pAct (the original human two-hybrid clone; nucleotides 1486–3525) into pGEX-5x-1 (Pharmacia Biotech, Inc.). GST-hBAP1(438–594) and pACT-hBAP1(438–594) (nucleotides 1486–1821) were generated and amplified by PCR, digested with restriction enzyme and ligated into the appropriate vector.

Mapping of BRCA1/BAP1 interaction domain

Truncations of mBAP(596–721), and the point mutation mBAP1(L691P), were generated by PCR-based mutagenesis. Products were then ligated into the mouse library-yeast expression vector, pVP16. All clones were confirmed by sequencing and expression in yeast was confirmed by Western analysis using antibodies against the VP16 activation domain (data not shown).

Northerns and in situ

Tissue RNA blots were obtained from Clontech Laboratories, Inc. (Palo Alto, CA). Blots were hybridized with ^{32}P-labeled hBAP1(483–729) cDNA (nucleotides 1486–3525) using standard protocols. RNA

preparation, Northern hybridization of mouse mammary tissue, and *in situ* hybridization analyses were performed as previously described using the mouse Bap1 cDNA probe described by mBAP1(596–721), corresponding to nucleotides 1825–2202 of the human probe (Marquis *et al.*, 1995).

Fluorescent *in situ hybridization (FISH)*

FISH using a biotin-labeled 3.5 kb cDNA (full length) clone of BAP1, with corresponding DAPI-banding and measurement of the relative distance from the short arm telomere to the signals (FLpter value) was performed as described previously (Tommerup and Vissing, 1995).

Immunolocalization

All immunofluorescence was performed as previously described (Ishov and Maul, 1996). BAP1 protein was detected with affinity purified, BAP1-specific polyclonal antibodies, and BRCA1 was detected with the BR64 monoclonal antibody (Upstate Biotechnology), which were detected with FITC and Texas Red (respectively) using biotin-avidin enhancement. Cells were stained for DNA with bis-benzimide (Hoescht 33258, Sigma Chemical Co.) and mounted using Fluoromount G (Fisher Scientific). Analysis was performed with a confocal scanning microscope (Leica, Inc.).

BAP1 protein characterization

Generation of antibodies: Using PCR cloning, the cDNA region encoding amino acids 483–576 of BAP1 was fused downstream of the six Histidine residues of the vector pQE-30 (QIAGEN Inc.). The His-tagged protein was purified from *E. coli* over a Ni-agarose column as previously described (Friedman *et al.*, 1996) and was used to immunize rabbits for the production of polyclonal antibodies (Cocalico Biologicals, Inc.). Immunoprecipitation of BAP1 was performed by previously described procedures for the metabolic labeling and immunoprecipitation of proteins from cell lysates (Friedman *et al.*, 1996).

In vitro protein association: GST, GST-hBAP1(483–729) and GST-hBAP1(483–594) were expressed in *E. coli* and then purified as described (Frangioni and Neel, 1993). The ^{35}S-BRCA1 protein was produced *in vitro* via coupled transcription/translation (TNT®, Promega Corp.). Association between proteins was assayed as described previously (Barlev *et al.*, 1995).

BAP1 enzymatic assay

Assays for BAP1 enzymatic activity were performed essentially as described for the UCH-L1 and UCH-L3 enzymes (Mayer and Wilkinson, 1989). Briefly, bacteria harboring an IPTG-inducible expression plasmid containing BAP1 (pQE-30; QIAGEN Inc.) were grown and induced with 1 mM IPTG for 4 h. The bacteria were collected and the pellets were resuspended to 1/20 volume (original culture) in lysate buffer (50 mM Tris, pH 8.0, 25 mM EDTA, 10 mM 2-mercapto-ethanol, 100 μg/ml lysozyme). The lysates were sonicated and centrifuged at 40 000 *g*. The soluble fractions were used for subsequent activity assays. The pellets were resuspended in a volume equal to that of the supernatant and samples of both pellet and supernatant were analysed by SDS–PAGE for expression levels and inclusion body formation.

Assays for ubiquitin carboxy-terminal hydrolase activity were performed using the glycine 76 ethyl ester of ubiquitin (Ub-OEt) as substrate (Mayer and Wilkinson, 1989; Wilkinson *et al.*, 1986). Assays were done in triplicate. The peak areas were integrated and normalized with respect to a ubiquitin standard.

Mutation screening

RNA/DNA preparation: Genomic DNA was prepared from breast and lung cancer cell lines using standard methods. Total RNA was extracted by the cesium chloride-ultracentrifugation method (Ausubel *et al.*, 1987). First strand cDNAs were synthesized from RNA by M-MLV reverse transcriptase (Gibco–BRL) according to the manufacturer's instructions.

Southern and Northern blot hybridization: Five μg of genomic DNA, subjected to restriction enzyme digestion, or 10 μg total RNA, was electrophoretically gel-fractionated and transferred to Hybond N$^+$ membranes (Amersham). Hybridization was performed with a ^{32}P-full-length BAP1 cDNA probe followed by washes under standard conditions and detection by autoradiography.

Single strand conformational polymorphism (SSCP) analysis: Seventeen overlapping PCR primer pairs, each with a predicted product size of approximately 200 base pairs, were designed to span the 2.2 kb open reading frame of the BAP1 cDNA sequence. cDNA (from RNA) was amplified in 20 μl PCR reactions containing 20 mM Tris HCl (pH 8.3), 50 mM KCl, 1.5 mM MgCl, 0.2 mM each dNTP, 0.1 mM each forward and reverse primer, 0.05 ml [^{32}P-α]dCTP and 0.5 units Taq DNA Polymerase (BRL). PCR reactions were carried out in a Perkin-Elmer 9600 Thermocycler using a touchdown technique: a 2.5 min initial denaturation at 94°C was followed by 35 cycles of denaturation at 94°C × 30 s, annealing, initially at 65°C decreasing by 1°C for each of the first ten cycles to 55°C, × 30 s, and extension at 72°C × 30 s with a final extension of 5 min at 72°C. PCR products were then diluted 1 : 10 with SSCP dye (95% formamide, 20 mM EDTA, and 0.05% each of bromophenol blue and xylene cyanol), heat-denatured, and electrophoresed on 0.5 × MDE gels ±10% glycerol. Abnormal single stranded DNA detected as autoradiographic shifts were re-amplified by PCR and subjected to automated dye-terminator sequencing (ABI 373).

References

Altschul SF, Gish W, Miller W, Myers EW and Lipman DJ. (1990). *J. Mol. Biol.*, **215**, 403–410.

Ausubel FM, Brent R, Kingston RE, Moore DD, Seidman JG, Smith JA and Struhl K. (1987). *Current Protocols in Molecular Biology*. John Wiley & Sons, Inc., Boston.

Barlev NA, Candau R, Wang L, Darpino P, Silverman N and Berger SL. (1995). *J. Biol. Chem.*, **270**, 19337–19344.

Borden KLB, Boddy MN, Lally J, O'Reilly NJ, Martin S, Howe K, Solomon E and Freemont PS. (1995). *EMBO J.*, **14**, 1532–1541.

Brown MT. (1995). *Gene*, **160**, 111–116.

Brown MT, Goetsch L and Hartwell LH. (1993). *J. Cell Biol.*, **123**, 387–403.

Buchhagen DL, Qiu L and Etkind P. (1994). *Int. J. Cancer*, **57**, 473–479.

Chapman MS and Verma IM. (1996). *Nature*, **382**, 678–679.

Chen CF, Li S, Chen Y, Chen PL, Sharp ZD and Lee WH. (1996a). *J. Biol. Chem.*, **271**, 32863–32868.

Chen Y, Chen CF, Riley DJ, Allred DC, Chen PL, Von Hoff D, Osborne CK and Lee WH. (1995). *Science*, **270**, 789–791.

Chen Y, Farmer AA, Chen CF, Jones DC, Chen PL and Lee WH. (1996b). *Cancer Res.*, **56**, 3168–3172.

Ciechanover A. (1994). *Biological Chemistry Hoppe-Seyler*, **375**, 565–581.

Couch FJ and Weber BL. (1996). *Hum. Mutat.*, **8**, 8–18.

Durfee T, Becherer K, Chen PL, Yeh SH, Yang Y, Kilburn AE, Lee WH and Elledge SJ. (1993). *Genes Dev.*, **7**, 555–569.

Easton DF, Bishop DT, Ford D and Crockford GP. (1993). *Am. J. Hum. Genet.*, **52**, 678–701.

Easton DF, Ford D, Bishop DT and Consortium T.B.C.L. (1995). *Am. J. Hum. Genet.*, **56**, 265–271.

Everett RD, Meredith M, Orr A, Cross A, Kathoria M and Parkinson J. (1997). *EMBO J.*, **16**, 566–577.

FitzGerald MG, MacDonald DJ, Krainer M, Hoover I, O'Neil, Unsal H, Silva-Arrieto S, Finkelstein DM, Beer-Romero P, Englert C, Sgroi DC, Smith BL, Younger JW, Garber JE, Duda RB, Mayzel KA, Isselbacher KJ, Friend SH and Haber DA. (1996). *N. Engl. J. Med.*, **334**, 143–149.

Ford D, Easton DF, Bishop DT, Narod SA and Goldgar DE. (1994). *Lancet*, **343**, 692–695.

Frangioni JV and Neel BG. (1993). *Anal. Biochem.*, **210**, 179–187.

Friedman JR, Fredericks WJ, Jensen DE, Speicher DW, Huang XP, Neilson EG and Rauscher III, FJ. (1996). *Genes & Development*, **10**, 2067–2078.

Futreal PA, Liu Q, Shattuck-Eidens D, Cochran C, Harshman K, Tavtigian S, Bennett LM, Haugen-Strano A, Swensen J, Miki *et al.* (1994). *Science*, **266**, 120–122.

Gray DA, Inazawa J, Gupta K, Wong A, Ueda R and Takahashi T. (1995). *Oncogene*, **10**, 2179–2183.

Gudas JM, Nguyen H, Li T and Cowan KH. (1995). *Cancer Res.*, **55**, 4561–4565.

Gudas JM, Tao L, Nguyen H, Jensen D, Rauscher III FJ and Cowan KH. (1996). *Cell Growth and Differentiation*, **7**, 717–723.

Hakem R, de la Pompa JL, Sirard C, Mo R, Woo M, Hakem A, Wakeham A, Potter J, Reitmair A, Billia F, Firpo E, Hui CC, Roberts J, Rossant J and Mak TW. (1996). *Cell*, **85**, 1009–1023.

Hall JM, Lee MK, Newman B, Morrow JE, Anderson LA, Huey B and King M-C. (1990). *Science*, **250**, 1684–1689.

Hedge AN, Inokuchi K, Pei W, Casadio A, Grirardi M, Chain DG, Martin KC, Kandel ER and Schwartz JH. (1997). *Cell*, **89**, 114–126.

Ho SN, Hunt HD, Horton RM, Pullen JK and Pease LR. (1989). *Gene*, **77**, 51–59.

Holt JT, Thompson ME, Szabo C, Robinson-Benion C, Arteaga CL, King M-C and Jensen RA. (1996). *Nature Genetics*, **12**, 298–302.

Honore B, Rasmussen HH, Vandekerckhove J and Celis JE. (1991). *FEBS Lett.*, **280**, 235–240.

Hu G, Zhang S, Vidal M, La Baer J, Xu T and Fearon ER. (1997). *Genes & Dev.*, **11**, 2701–2714.

Huang Y, Baker RT and Fischer-Vize JA. (1995). *Science*, **270**, 1828–1831.

Huang Y and Fischer-Vize JA. (1996). *Development*, **122**, 3207–3216.

Inouye C, Dhillon N and Thorner J. (1997). *Science*, **278**, 103–106.

Isaksson A, Musti AM and Bohmann D. (1996). *Biochimica et Biophysica Acta*, **1288**, F21–F29.

Ishov AM and Maul GG. (1996). *J. Cell Biol.*, **134**, 815–826.

Jiang W and Koltin Y. (1996). *Mol. Gen. Genet.*, **251**, 153–160.

Jin Y, Xu XL, Yang M-CW, Wei F, Ayi T-C, Bowcock AM and Baer R. (1997). *Proc. Natl. Acad. Sci. USA*, **94**, 12075–12080.

Johnston SC, Larsen CN, Cook WJ, Wilkinson KD and Hill CP. (1997). *EMBO J.*, **16**, 3787–3796.

Klug A and Schwabe JW. (1995). *FASEB J.*, **9**, 597–604.

Kok K, Hofstra R, Pilz A, van den Berg A, Terpstra P, Buys CH and Caritt B. (1993). *Proc. Natl. Acad. Sci. USA*, **90**, 6071–6075.

Koonin EV, Altschul SF and Bork P. (1996). *Nature Genet.*, **13**, 266–268.

Lam YA, Xu W, DeMartino GN and Cohen RE. (1997). *Nature*, **385**, 737–740.

Larsen CN, Price JS and Wilkinson KD. (1996). *Biochem.*, **35**, 6735–6744.

Lennon GG, Auffray C, Polymeropoulos M and Soares MB. (1996). *Genomics*, **33**, 151–152.

Liu CY, Flesken-Nikitin A, Li S, Zeng Y and Lee WH. (1996). *Genes & Dev.*, **10**, 1835–1843.

Lovering R, Hanson IM, Borden KL, Martin S, O'Reilly NJ, Evan GI, Rahman D, Pappin DJ, Trowsdale J and Freemont PS. (1993). *Proc. Natl. Acad. Sci. USA*, **90**, 2112–2116.

Madden SL, Cook DM, Morris JF, Gashler A, Sukhatme VP and Rauscher III, FJ. (1991). *Science*, **253**, 1550–1553.

Mahajan R, Delphin C, Guan T, Gerace L and Melchoir F. (1997). *Cell*, **88**, 97–107.

Marks JR, Huper G, Vaughn JP, Davis PL, Norris J, McDonnell DP, Wiseman RW, Futreal PA and Iglehart JD. (1997). *Oncogene*, **14**, 115–121.

Marquis ST, Rajan JV, Wynshaw-Boris A, Xu J, Yin GY, Abel KJ, Weber BL and Chodosh LA. (1995). *Nature Genet.*, **11**, 17–26.

Mayer AN and Wilkinson KD. (1989). *Biochemistry*, **28**, 166–172.

Merajver SD, Pham TM, Caduff RF, Chen M, Poy EL, Cooney KA, Weber BL, Collins FS, Johnston C and Frank TS. (1995). *Nat. Genet.*, **9**, 439–443.

Miki Y, Swensen J, Shattuck-Eidens D, Futreal PA, Harshman K, Tavtigian S, Liu Q, Cochran C, Bennett LM, Ding W *et al.* (1994). *Science*, **266**, 66–71.

Moazed D and Johnson D. (1996). *Cell*, **86**, 667–677.

Muto MG, Cramer DW, Tangir J, Berkowitz R and Mok S. (1996). *Cancer Res.*, **56**, 1250–1252.

Nakamura T, Hillova J, Mariage-Samson R, Onno M, Huebner K, Cannizzaro LA, Boghosian-Sell L, Croce CM and Hill M. (1992). *Oncogene*, **7**, 733–741.

Papa FR and Hochstrasser M. (1993). *Nature*, **366**, 313–319.

Patarca R, Freeman GJ, Schwartz J, Singh RP, Kong QT, Murphy E, Anderson Y, Sheng FY, Singh P, Johnson KA *et al.* (1988). *Proc. Natl. Acad. Sci. USA*, **85**, 2733–2737.

Phelps RM, Johnson BE, Ihde DC, Gazdar AF, Carbone DP, McClintock PR, Linnoila RI, Matthews MJ, Bunn Jr, PA, Carney D, Minna JD and Mulshine JL. (1996). *J. Cell Biochem. Suppl.*, **24**, 32–91.

Rao VN, Shao N, Ahmak M and Reddy ESP. (1996). *Oncogene*, **12**, 523–528.

Rechsteiner M and Rogers SW. (1996). *Trends Biochem. Sci.*, **21**, 267–271.

Roa BB, Boyd AA, Volcik K and Richards CS. (1996). *Nature Genet.*, **14**, 185–187.

Saitoh H, Pu RT and Dasso M. (1997). *Trends Biochem. Sci.*, **22**, 374–376.

Saurin AJ, Borden KLB, Boddy MN and Freemont PS. (1996). *Trends Biochem. Sci.*, **21**, 208–214.

Scully R, Anderson SF, Chao DM, Wanjiang W, Liyan Y, Young RA, Livingston DM and Parvin JD. (1997a). *Proc. Natl. Acad. Sci. USA*, **94**, 5605–5610.

Scully R, Chen J, Plug A, Xiao Y, Weaver D, Feunteun J, Ashley T and Livingston DM. (1997b). *Cell*, **88**, 265–275.

Scully RSG, Brown M, Caprio JAD, Cannistra SA, Feunteun J, Schnitt S and Livingston DM. (1996). *Science*, **272**, 123–126.

Sellers WR and Kaelin WG. (1996). *Biochim. Biophys. Acta*, **1288**, M1–5.

Shen Z, Pardington-Purtymun PE, Comeaux JC, Moyzis RK and Chen DJ. (1996a). *Genomics*, **37**, 183–186.

Shen Z, Pardington-Purtymun PE, Comeaux JC, Moyzis RK and Chen DJ. (1996b). *Genomics*, **36**, 271–279.

Smith SA, Easton DG, Evans DGR and Ponder BAJ. (1992). *Nature Genetics*, **2**, 128–131.

Struewing JP, Abeliovich D, Peretz T, Avishai N, Kaback MM, Collins FS and Brody LC. (1995). *Nature Genetics*, **11**, 198–200.

Szabo CI and King M-C. (1995). *Hum. Mol. Genet.*, **4**, 1811–1817.

Thakur S, Zhang HB, Peng Y, Le H, Carroll B, Ward T, Yao J, Farid LM, Couch FJ, Wilson RB and Weber BL. (1997). *Mol. Cell. Biol.*, **17**, 444–452.

Thiberville L, Bourguignon J, Metayer J, Bost F, Diarra-Mehrpour M, Bignon J, Lam S, Martin JP and Nouvet G. (1995). *Int. J. Cancer*, **64**, 371–377.

Thompson JD, Higgins DG and Gibson TJ. (1994). *Nucleic Acids Res.*, **22**, 4673–4680.

Thompson ME, Jensen RA, Obermiller PS, Page DL and Holt JT. (1995). *Nat. Genet.*, **9**, 444–450.

Tommerup N and Vissing H. (1995). *Genomics*, **27**, 259–264.

Vaughn JP, Davis PL, Jarboe MD, Huper G, Evans AC, Wiseman RW, Berchuck A, Iglehart JD, Futreal A and Marks JR. (1996). *Cell Growth Differ.*, **7**, 711–715.

Vojtek AB, Hollenberg SM and Cooper JA. (1993). *Cell*, **74**, 205–214.

Watkins JF, Sung P, Prakash L and Prakash S. (1993). *Mol. Cell. Biol.*, **13**, 7757–7765.

Welch PJ and Wang JY. (1995). *Genes Dev.*, **9**, 31–46.

Wilkinson KD. (1995). *Ann. Rev. Nutrition*, **15**, 161–189.

Wilkinson KD, Cox MJ, Mayer AN and Frey T. (1986). *Biochemistry*, **25**, 6644–6649.

Wilkinson KD, Deshpande S and Larsen CN. (1992). *Biochem. Soc. Trans.*, **20**, 631–637.

Wilkinson KD, Lee KM, Deshpande S, Duerksen-Hughes P, Boss JM and Pohl J. (1989). *Science*, **246**, 670–673.

Wu LC, Wang ZW, Tsan JT, Spillman MA, Phung A, Xu XL, Yang MC, Hwang LY, Bowcock AM and Baer R. (1996). *Nature Genet.*, **14**, 430–440.

Zabludoff SD, Wright WW, Harshman K and Wold BJ. (1996). *Oncogene*, **13**, 649–653.

Zhu Y, Carroll M, Papa FR, Hochstrasser M and D'Andrea AD. (1996). *Proc. Natl. Acad. Sci. USA*, **93**, 3275–3279.

Zhu Y, Lambert K, Corless C, Copeland NG, Gilbert DJ, Jenkins NA and D'Andrea AD. (1997). *J. Biol. Chem.*, **272**, 51–57.